

ORGANISATION EUROPÉENNE POUR LA RECHERCHE NUCLÉAIRE
CERN EUROPEAN ORGANIZATION FOR NUCLEAR RESEARCH

Fifty years of the CERN Proton Synchrotron

Volume II

Editors: S. Gilardoni
D. Manglunki

ISBN 978-92-9083-391-8

ISSN 0007-8328

DOI 10.5170/CERN-2013-005

Copyright © CERN, 2013

© Creative Commons Attribution 3.0

Knowledge transfer is an integral part of CERN's mission.

CERN publishes this report Open Access under the Creative Commons Attribution 3.0 license (<http://creativecommons.org/licenses/by/3.0/>) in order to permit its wide dissemination and use.

This monograph should be cited as:

Fifty years of the CERN Proton Synchrotron, volume II

edited by S. Gilardoni and D. Manglunki, CERN-2013-005 (CERN, Geneva, 2013),

DOI: 10.5170/CERN-2013-005

Dedication

The editors would like to express their gratitude to Dieter Möhl, who passed away during the preparatory phase of this volume. This report is dedicated to him and to all the colleagues who, like him, contributed in the past with their cleverness, ingenuity, dedication and passion to the design and development of the CERN accelerators.

Abstract

This report sums up in two volumes the first 50 years of operation of the CERN Proton Synchrotron. After an introduction on the genesis of the machine, and a description of its magnet and powering systems, the first volume focuses on some of the many innovations in accelerator physics and instrumentation that it has pioneered, such as transition crossing, RF gymnastics, extractions, phase space tomography, or transverse emittance measurement by wire scanners. The second volume describes the other machines in the PS complex: the proton linear accelerators, the PS Booster, the LEP pre-injector, the heavy-ion linac and accumulator, and the antiproton rings.

Preface

It was on 24 November 1959 that the proton beam in the CERN Proton Synchrotron was accelerated to a kinetic energy of 24 GeV. Thus the first strong-focusing proton synchrotron ever built has been faithfully serving the international physics community for 50 years. It has been the subject of a virtually continuous upgrade boosting its intensity per pulse from 10^{10} protons by more than three orders of magnitude to 3×10^{13} protons. Various injectors have been added and it has been modified such that, in addition to protons, light and heavy ions, positrons and electrons, as well as antiprotons could be accelerated or even decelerated often within the same supercycle. This would not have been possible had the initial design not been solid and sound allowing for maintainability, flexibility, and versatility and whose intrinsic potential was brought to fruition by the efforts and the ingenuity of generations of accelerator physicists, engineers, operators, and technicians. This report has been written to mark the fiftieth anniversary of the first operation of this unique accelerator. Volume I outlines the euphoric spirit in the European physics community in which such a bold design could be suggested, and gives an overview of the evolution of this unique accelerator described in a wealth of publications. This volume provides also a description in more depth of the outstanding achievements and highlights in its development. Volume II provides an overview of the injectors of the PS and of the accelerator system used for antiproton accumulation and storage, which has been closely associated with the PS.

Contributors

Jean-Paul Burnet, Christian Carli, Michel Chanel, Roland Garoby, Simone Gilardoni, Massimo Giovannozzi, Steven Hancock, Helmut Haseroth, Kurt Hübner, Detlef Küchler, Julian Lewis, Alessandra Lombardi, Django Manglunki, Michel Martini, Stephan Maury, Elias Métral, Dieter Möhl, Günther Plass, Louis Rinolfi, Richard Scrivens, Rende Steerenberg, Charles Steinbach, Maurizio Vretenar, Thomas Zickler

Contents

| | |
|---|-----|
| Preface | vii |
| List of contributors | ix |
| Linac 1 | 1 |
| The Proton Synchrotron Booster (PSB) | 7 |
| Linac 2 | 15 |
| The Antiproton Accumulator, Collector and Decelerator Rings | 21 |
| The Low-Energy Antiproton and Ion Rings LEAR and LEIR | 33 |
| The LEP Pre-injector (LPI) | 47 |
| Linac 3 | 53 |

Linac 1

1 Introduction

The CERN Linac 1 was originally designed in the early 1950s to serve as injector for the Proton Synchrotron (PS). CERN's original proton linear accelerator (linac) accelerated its first beam in 1958 and was fully commissioned in 1959 when one turn of 50 MeV protons went round the PS. It was the only supplier of protons to the CERN synchrotrons until Linac 2 took over in 1978. It was used also for the acceleration of light ions (deuterons, alpha particles and partially stripped oxygen and sulphur ions as well as H^- ions).

2 Machine layout

The design of Linac 1 [1] was based on a similar accelerator built for the Atomic Energy Research Establishment (known as AERE or colloquially Harwell) at Harwell in England. In April 1958, tank 1 produced the first 10 MeV proton beam with an intensity of (20–25) μA from an input beam, produced by a radiofrequency (RF)-type ion source, of 2 mA. Later that year the input intensity was brought to 20 mA (improved steering and focusing) and the output intensity to (250–300) μA (change in RF tank level flatness and tilt).

The basic layout consisted of three Alvarez-type accelerators (up to 10 MeV, 30 MeV and 50 MeV), each RF resonator housed inside an external vacuum tank, built by Metropolitan Vickers (Fig. 1). It ran at a frequency of 202.56 MHz, related to wartime radar developments. Grid focusing in the first Alvarez resonator was originally foreseen, but new drift tubes with pulsed quadrupoles were eventually installed; the RF ion source produced originally some microseconds pulse length. The RF power was generated by triodes in glass technology (FTH-470) with 2 MW peak power and fed by delay-line-type modulators, switched with ignitrons. Injection into the first tank was done with the source sitting at a high-voltage (HV) terminal with 520 kV (Fig. 2), the HV generator built by Haefely using a Greinacher cascade running at 50 Hz.

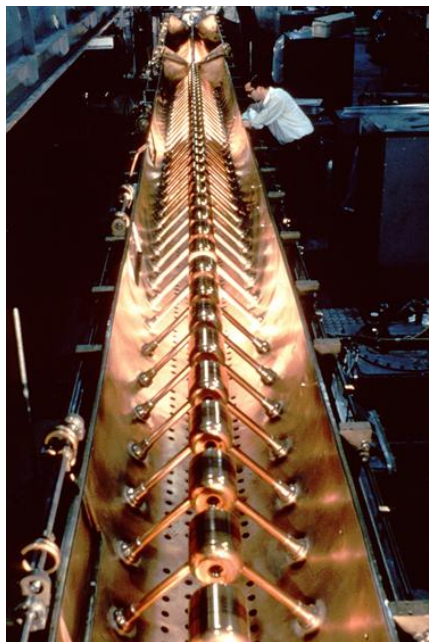


Fig. 1: Open Linac 1 Alvarez tank



Fig. 2: The 520 kV Linac 1 HV generator

3 Improvements and operation for the Proton Synchrotron Booster

The initial improvements eventually resulted in an output beam of up to 4.8 mA at 50 MeV and in September 1959 the first turn at that energy went around the PS (6.7 μ s being required for single turn injection).

In the early 1960s, rapid development was resulting in an increase of the operational peak currents from 5 mA to greater than 50 mA and a pulse length up to 20 μ s. There were improvements to the RF ion source, the gradient in the pre-injector increased, larger aperture quadrupoles were installed and better beam matching using two triplets in the Low Energy Beam Transport (LEBT) was achieved. Important developments in the ancillary equipment were extra modulators and RF feedforward coupling loops to compensate for transient beam loading, and the start of serious investigations into beam quality, especially transverse emittances and beam brightness.

After the installation of a duoplasmatron source and a very high-gradient two-gap, re-entrant pre-injector, a peak performance of 135 mA in 20 μ s was achieved.

The HV column used a new design with a high-gradient gap interrupted by an intermediate electrode using porcelain rings glued with araldite and some resistors on the outside to produce a constant gradient to avoid air breakdown.

However, the long-term aim was to meet the high-quality requirements of the Proton Synchrotron Booster (PSB) input beam of 100 mA, 100 μ s for multiturn injection [2].

Improvements and consolidation stages were first concerned with the HT compensation (bouncer) to compensate for the drop in the accelerating voltage due to beam loading. The previous passive compensation by means of a programmed spark gap was replaced with a feedback regulation by means of a HV electronic tube.

Lengthening of the quadrupole pulses in the first tank was also required, with quadrupoles in tanks 2 and 3 being run on DC supplies. This was achieved by adding a higher harmonic to the capacitive discharge circuit. Tests were done with multiturn (three or four turns) injection into the PS.

To cope with the longer pulses and to achieve the necessary small energy spread for the PSB a double debuncher arrangement was installed. Detailed beam studies resulted in the installation of single-pulse emittance and energy spread measurements at the hand-over point of the beam. Among the changes to improve operational reliability were the replacement of mercury diffusion pumps and their liquid-nitrogen-cooled baffles by high-speed turbo-molecular pumps. This investment paid for itself within a few years due to the enormous savings in electrical power and cooling water. The typical operational results at 50 MeV were about 70 mA for 100 μ s.

These long pulses were only possible with an extended upgrade of the RF system with a complicated distribution of RF power to main amplifiers and compensation amplifiers to compensate for the beam loading of the high-intensity beams. Installation of phase shifters to allow for independent adjustments of phases between the different amplifiers and installation of circulators were needed to provide some isolation in the RF network. RF beam loading compensation amplifiers used higher-power tubes (FTH 516) to cope with the higher currents.

4 Protons, deuterons, alphas and a radiofrequency quadrupole

It is clear that a machine designed in 1954 had difficulties in meeting the demands made in the 1970s by the PSB.

Machine limitations were in input matching, especially in longitudinal phase space. With a low injection energy (520 keV) only $++--$ focusing was possible in Linac 1 and for high currents the poor RF field transient behaviour due to unstabilized structures was evident. The RF cavities embedded in a vacuum vessel were neither suitable for modern high-vacuum technology nor for stable alignment. The ancillary equipment, which lacked modern performance capabilities, including the RF system (without feedback for level or phase control), the control system and the measuring gear were not, in spite of even further increases of the beam current, optimal for the PSB. Therefore, the decision had been taken to build a new modern linac (Linac 2) as replacement for Linac 1, with a study starting in 1973. This linac was ready at the end of 1978 and started regular operation in 1979.

As the only injector for the PSB and the PS, Linac 1 needed to be kept operational with high performance and good reliability. Nevertheless machine studies for deuteron acceleration were already started in 1964 using the $2\beta\lambda$ mode instead of the $\beta\lambda$ mode. This mode accelerates the particles with half the velocity, hence starting with a pre-injector voltage at 260 kV and with about the same RF fields, due to the bad transit time factor. Acceleration with the same speed as for protons was obviously not possible because an increase in all electrical and magnetic fields was just too far beyond the technical possibilities. Again due to the bad transient time factor in the $2\beta\lambda$ mode the RF resonator in tank 1 had to be “tilted”, i.e. operated with a higher field in the beginning of the resonator, to achieve a good transmission. This operation was not easy in a machine that had to run reliably most of the time for its “proton customers” [3].

During the 1970s the use of Linac 1 for accelerating deuterons was continued, encouraged by a small part of the physics community. After years of improvement (higher intensities and longer pulses), deuterons were accelerated and then stacked in the CERN Intersecting Storage Rings (ISR) for use in physics experiments and a run in 1976 resulted in the production of deuteron beams at a reasonable intensity (above 10 mA) for acceleration in the PS and subsequent stacking in the ISR. Of course the focusing in the linac had to be adapted and the machine was run with a $+-$ focusing in the first tank instead of the $++--$ focusing as for protons. The success of this operation was followed by some trials with alpha particles and prompted finally a request for alpha particles in the ISR.

If the source had supplied a reasonable intensity of He^{2+} ions, then acceleration in the linac would have caused no more problems than deuteron acceleration, as the charge/mass ratio is the same. Unfortunately, a duoplasmatron is not really suitable for the production of an intense He^{2+} beam. The solution was finally to accelerate from the pre-injector a He^{1+} beam with the normal 520 kV, thus producing a beam with half the proton velocity (i.e. with the same velocity of the deuterons at 260 kV) and stripping this beam to achieve a He^{2+} beam. Doing this at low energy is tricky, as the thickness of the stripper needs to be very low. A stripping foil would not be feasible, only a gas stripper could be used. A normal gas stripper would have increased the gas load for the vacuum pumps by several orders of magnitude. Hence, a pulsed gas stripper was adopted using a pulsed piezoelectric valve to fill for a very short time (about a millisecond) a tube that the He^{1+} beam had to pass through. Stripping efficiencies of 30% at this low energy were achieved and resulted in some 10 mA of alpha particles at the end of the linac, giving adequate intensities to the ISR in 1980 [4, 5].

The success of this operation and the potential of fixed target physics with ions launched the programme for physics at Super Proton Synchrotron (SPS) energies with oxygen and heavier ions.

Another important development was a radiofrequency quadrupole (RFQ) designed to replace the old 500 kV Cockcroft/Walton and high-gradient pre-injector column. It was successfully installed in front of Linac 1 in 1984 and gave an output beam of 80 mA protons at 520 keV of which 65 mA were taken to 10 MeV [6–8]. Unfortunately, this installation inhibited further use of deuteron or alpha beams for the time being.

Test beams for the Low Energy Antiproton Ring (LEAR) with proton (and H^-) beams started again around 1983.

5 Oxygen and sulphur

Moving back of the whole linac by some 12 m to allow for sufficient shielding towards the ejected beams from the PS became necessary because of the ever-increasing beam intensities of the PS (Fig. 3). The old pre-injector Faraday cage was disassembled; a 5 m shielding wall could then be installed downstream. The full proton beam with the RFQ was re-established in March 1985. This was a huge enterprise but was required to install another RFQ and an electron cyclotron resonance (ECR) source for oxygen ions installed in collaboration with LBL, Berkeley, GSI, Darmstadt, and CEN, Grenoble (Fig. 4). The switch from deuteron and alpha beams to oxygen was a strong request from the physics community. The first idea was to use the ISR, but the dismantling of this machine pushed the newly requested beams to the SPS.

The ECR source was not able to supply fully stripped oxygen ($8+$), but only a 25% lower charge-to-mass ratio ($6+$). This low charge state needed therefore 33% higher fields (RF and focusing) as compared with deuterons or alpha particles. In particular, to reach 33% higher RF fields, the RF generators were pushed to the limit and required a fairly substantial upgrade. The other problem was that 33% higher RF fields in the cavities were almost impossible, because of breakdown. The solution was a thorough cleaning, especially of tank 1, with the removal of as much of the plastic material between the resonator and the vacuum vessel as possible, without hampering too much the functioning of the tank. Additional pumping by means of a high-speed cryo-pump proved essential. Conditioning of the RF could only be done with the help of a carefully designed computer program, which would run for weeks to achieve the desired levels.



Fig. 3: Moving back Linac 1

The reward for this effort was the successful acceleration of oxygen ions in September 1986 [9]. Later followed a switchyard to allow for either injection of ions into the Booster or test beams for LEAR with either protons or H^- ions, subsequently upgraded for sulphur $12+$ ions (Fig. 4). After upgrading the ECR source, the first successful run with sulphur ions took place in 1987 [10].

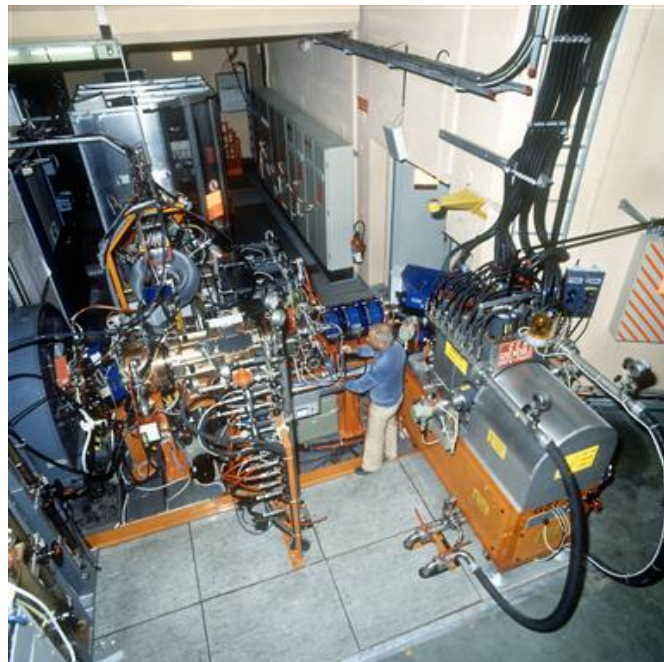


Fig. 4: The double Linac 1 pre-injector (oxygen and protons)

6 Conclusions

CERN's original proton linac accelerated its first beam in 1958 and was fully commissioned in 1959 when one turn of 50 MeV protons went round the PS. It was the only supplier of protons to the CERN synchrotrons until Linac 2 took over in 1978. Between that date and its final retirement in the summer of 1992 (after 33 years of service), it not only continued to supply protons for machine experiments, it was also used to accelerate alpha particles, deuterons and oxygen, sulphur and H⁻ ions. Oxygen and sulphur ions required a 33% increase in the design accelerating and focusing fields. In addition, the linac acted as a test bed for the first RFQ experiments. It was moved backwards by some 12 m to facilitate the ion acceleration tests and to install adequate radiation shielding towards the PS and its ejected beams. Eventually it was provided with two new injectors, protons from a duoplasmatron and via the RFQ for LEAR tests, and light ions (oxygen and sulphur) for SPS fixed target physics. Although exposed to many modifications for improvement it continued its faithful operation until retirement after 33 years of service [11, 12].

Ion production had been taken over by Linac 3 in 1994. Finally, Linac 1 was dismantled in 1992 with the RF resonator in tank 1 being exposed in the Microcosm.

References

- [1] E. Regenstreif, The CERN Proton Synchrotron (2nd Part), CERN 60-26 (1960).
- [2] H. Haseroth and P. Têtu, Recent operation and modifications on the CPS-50 MeV Linac (old Linac), Proc. 1976 Proton Linear Accelerator Conf., Chalk River, ON, Canada, AECL-5677, 1976.
- [3] P. Asboe-Hansen *et al.*, Acceleration and stacking of deuterons in the CERN PS and ISR, Proc. 7th US Particle Accelerator Conf., Chicago, IL, 1977 [IEEE Trans. Nucl. Sci. **NS-24** (1977) 1557].
- [4] M. Boutheon *et al.*, Acceleration and stacking of α -particles in the CERN Linac, PS and ISR, Proc. 9th US Particle Accelerator Conf., Washington, DC, 1981 [IEEE Trans. Nucl. Sci. **NS-28** (1981) 2049].
- [5] H. Haseroth, Light ions in the PS complex, CERN/PS/LR/ 81-27 (1981).
- [6] E. Boltezar *et al.*, Experimental RFQ as injector to CERN Linac I, Proc. 1981 Linear Accelerator Conf., Santa Fe, NM, 19–23 October 1981.
- [7] E. Boltezar *et al.*, Status and first beam measurements on the CERN RFQ, Proc. 12th Int. Conf. on High-Energy Accelerators, Fermilab, Batavia, IL, 11–16 August 1983.
- [8] E. Boltezar *et al.*, Performance of the CERN RFQ (RFQ1 Project), Proc. 1984 Linear Accelerator Conference, Seeheim, Germany, 7–11 May 1984.
- [9] H. Haseroth *et al.*, Ion acceleration in the CERN Linac 1, in Proc. 1986 Linear Accelerator Conf., Stanford, CA, 2–6 June 1986.
- [10] N. Angert *et al.*, Accelerating and separating mixed beams of ions with similar charge to mass ratio in the CERN PS complex, CERN/PS 88-29 HI, Proc. 1st EPAC Conf., Rome, Italy, 7–11 June 1988.
- [11] H. Haseroth *et al.*, History, developments and recent performance of the CERN Linac 1, Proc. 1992 Linac Conf., Ottawa, Canada, 23–28 August 1992.
- [12] H. Haseroth, *Phys. Rep.* **403-404** (2004) 27.

The Proton Synchrotron Booster (PSB)

1 Introduction

In the mid-1960s, as CERN's new 28 GeV Proton Synchrotron (PS) was getting into its stride, plans were being prepared for the next stage of CERN development. Ideas for new machines [1], which would eventually become the Intersecting Storage Rings (ISR) and the Super Proton Synchrotron (SPS), were in the air.

As the new machine debate continued, a clear requirement emerged to boost the proton yield to 10^{13} protons per PS pulse. This would provide more punch for the ongoing physics programme, then eclipsed by achievements on the other side of the Atlantic, and prepare the way to what would come later.

Plans gradually focused on a multiring slow cycling machine, in which particles from the individual rings could be combined to inject a dense beam into the PS. An initial proposal foresaw an Olympic five-ring machine, but this was discarded for a more modest, and at the same time more flexible, four-ring design [2, 3]. In this machine, measuring one quarter of the PS circumference of 628 m, the particles from each ring are transferred one after the other to fill the PS in one pulse.

Construction started in 1968, with the centre of the machine lying exactly on the Franco–Swiss border of the newly enlarged CERN site. The different regulations of the two CERN host states led to the decision to accommodate the visible Proton Synchrotron Booster (PSB) infrastructures on the Swiss side rather than on the French side.

On 26 May 1972 the PSB accelerated its first particles to the 800 MeV design energy. Experiments did not have to wait long for the payoff, and in 1973 the neutral current search at the Gargamelle bubble chamber benefited from the increased proton supply from the PS. The following year the PSB attained its design goal of 10^{13} particles per pulse (2.5×10^{12} per ring).

Then the time started for continuous improvements of beam quality and performance [4, 5]. Amongst those, it is worth noticing the constant fight against longitudinal or transverse instabilities, the improvement of injection efficiency, the search for the best dynamic working point in the tune diagram, the decrease of the tune spread, the transverse acceptance, the adaptation to the new Linac 2 and last but not least the compensation of beam loading. All these improvements allowed to accelerate more than 10^{13} protons per ring to the top energy with a record of $4.25 \cdot 10^{13}$ for the four rings together.

In 1992, on its 20th anniversary, the PSB received ISOLDE (On-Line Isotope Mass Separator) as a present [6, 7]. It was no longer the only synchrotron at CERN without an experimental area. To increase the performance of the PS and to make better use of the beams in the ISOLDE experiments, the extracted beam energy was pushed to 1 GeV without major difficulties.

Then in 1993 came the preparation for the next stage in its career, the PSB being the first of a fourfold chain of synchrotrons culminating in the CERN Large Hadron Collider (LHC) proton collider. The special LHC requirements, with beam brilliances twice the current level, requires special gymnastics to beat space-charge defocusing. For the LHC, the PSB delivers two-batch filling to the PS, injecting the four bunches from its four rings into one half of the PS circumference. With the first batch having to wait for the second, the PSB obligingly increased its energy from 1 GeV to 1.4 GeV to reduce unwelcome space-charge effects [8 – 11].

During all of this time, it also provided different ions species to the PS, beginning with deuterium and alpha particles in the early 1980s and gradually making its way up the periodic table to reach lead in 1994.

2 From design to start-up

2.1 Which machine to build [12]

2.1.1 *A Linac*

A Linear accelerator at higher energy was deemed much too expensive compared to a synchrotron even with many superimposed rings.

2.1.2 *Rapid Cycling Synchrotron*

Having chosen three or four rings/injection, single-turn extraction and injection into the main ring, the disadvantages of the Rapid Cycling Synchrotron (RCS; such as longer filling time, complications of the design of magnet power supply, RF system, vacuum chamber, etc.) appeared too important compared with the disadvantages of three or four superimposed or interlaced rings (multiplication of components). Another argument was that the staff available had no experience with resonant power supplies and not enough time to gain experience. On the other hand, the problems associated with a slow cycling booster looked easier. In particular, the problem of placing the bunches from the three or four rings into the same RF bucket of the PS ring appeared less difficult.

2.1.3 *The Number of Rings*

After a long discussion, the choice was given to study with the highest priority the four superimposed booster rings. It fulfilled the previously mentioned conditions without a loss of bunches as in the three-ring case. In addition, the PS was able to accelerate 1.6×10^{12} ppp and only a factor of six would have to be gained to reach the 10^{13} ppp (4 coming from the 4 rings having a length of $\frac{1}{4}$ of the PS, then $\frac{1}{4}$ of the space-charge detuning and 1.5 for the number of particles per ring in the same emittance). Another constraint was the possibility to fill the ISR with 10 or 5 buckets, and the four-ring solution eased this kind of operation. Therefore, this choice was considered as reasonable.

2.2 Lattice parameters

The extraction energy of 800 MeV was chosen to increase the space-charge limit by a factor of eight (the same normalized emittances with at least six times the intensity). It was also noted that two rings from the PSB could be extracted simultaneously and superimposed in the extraction line to double the bunch intensity into the PS when filling half the circumference in one pulse. This energy was also a compromise between the 600 MeV originally selected and the 1 GeV machine which would have been the best solution for the ISR.

The choice of four rings leads directly to the machine radius of 25 m. After having studied carefully the possibilities of magnet lattices with no systematic resonances within a stability diamond of $\Delta Q = 1$, designers came to the resulting choice of 16 periods and $4 < Q < 5$ without superperiodicity [13].

The wish to vary the tune Q by about $\pm 10\%$ without using the somewhat inconvenient pole face windings has led to adopt a separate function design. The C-type magnet located on either side of the long straight section greatly facilitated beam injection and ejection. Selection of a triplet for focusing led to rather small $\beta_{h,v}$ values inside the bending magnets, advantageous because of the reduction of the total height of the four rings and the limited power consumption permitting direct pulsing from the local electricity grid (the beam separation was finally set to 360 mm, limited by the ferrite rings of the RF cavities). It also eased specifications for the equipment in the long straight sections (kickers, septa, RF). The parameters of the triplets have been optimized by minimizing notably the following effects: closed orbit distortions, influence of the lens fringe field and Q -shifts due to betatron amplitudes [14 – 16].

2.3 Construction

The dipole magnets and quadrupole triplets were finally designed in such a way to be powered with the same power supply with only two trims on QF and QD. In addition, the cabling of the external gaps of the bending was separated from the internal ones, which allowed a virtual ‘ground’, a limited voltage to ground and, last but not least, would allow the trimming of the external gaps in case of their potentially different behaviour. Of course long discussions have taken place to specify the positions of the elements such as the correction dipoles in section L3, the pick-ups (ceramics) inside the correcting multipole elements in L2, the vacuum fast connecting and insulating flange or the position of the RF cavities (which offered the possibility to have another one installed in the opposite straight section and to further let the beam debunch from the injection to the cavity).

2.4 Start-up

The running-in started in May 1972. The start-up with beam went quite smoothly, as was reported already in October 1972 [17] that the highest intensity accelerated to 800 MeV in any ring was 1.4×10^{12} protons, about half the nominal value. The design intensity was reached in 1973, and finally 10^{13} protons were accelerated in the PS in 1974.

3 The improvement time

3.1 General review [18]

Starting from the rather modest performances, the PSB has now surpassed four times the design intensity [19] (see Fig. 1), featuring the maximum space-charge limit of 0.6 units. The latter requires dynamic compensation of half and (even systematic) third integer stop bands. Other measures were introduced to push the intensity to higher values: careful choice of working area; control linear coupling to enhance injection efficiency and fill the transverse aperture with a better suited transverse distribution; bunch shaping by the addition of a second harmonic RF system; feedback system taming coupled bunch instabilities; and transverse wide-band dampers replacing octupoles used previously. In addition there were two major changes in the PSB: to push the space-charge limit at PS injection, the PSB extraction energy was increased to 1 GeV [20] and later to 1.4 GeV; for the LHC filling, the PSB RF system was completely changed from the original $h = 5 + 10$ harmonics to the currently used $h = 1 + 2$ harmonics.

3.2 Increasing the space-charge limit

Space charge remains the ultimate limit to intensity in low-energy machines. The expression for the space-charge limit, essentially due to Laslett, is fundamental to all attempts to push the intensity:

$$\Delta Q_y = \frac{N r_p}{\pi \beta^2 \gamma^3 \epsilon_y} \frac{G F_y}{H_y B_f}$$

where B_f is the bunching factor (equal to average/peak intensity), ϵ_y , ϵ_x are the physical emittances in the x - y plane, F_y corrects for image force ~ 1 and G is the form factor accounting for transverse density distribution, $G = 1(2)$ for uniform (Gaussian) density in the x - y plane and, finally,

$$H_y = \langle (1 + \sqrt{(\epsilon_x \beta_x + (D \frac{\Delta p}{p})^2)}) / \sqrt{\epsilon_y \beta_y} \rangle$$

represents the aspect ratio of the beam averaged over a superperiod.

To maximize the number of protons, all of the factors should be optimized. This is what has been done since the start of the PSB except that the injection energy (β, γ) and the vacuum chamber and magnet poles (F_y) have not been changed. It should be noted that each time the space-charge limit was improved, occurring instabilities had to be cured.

3.2.1 *Working area*

Under the influence of space charge, the beam occupies a necktie in the tune diagram. Consequently fewer stop bands intercept with this shape in the lower left-hand corner than in the others. The change from the original working point to the quadrant chosen ($Q_{x,y} = 4.2, 5.3$) coincides also with the minimum of H_y . Later on it was found that the systematic third-order resonance $3Q_y = 16$ limits the performance of the outer rings, and the lower quadrant ($Q_{x,y} = 4.2, 4.3$) was chosen despite the increase of H_y , the presence of the Montague coupling resonance $2Q_x - 2Q_y = 0$ and the systematic resonance $4Q_{x,y} = 16$.

3.2.2 *Dynamic working point*

The Laslett tune shift decreases with $\beta\gamma^2$ in the absence of beam blow-up. This suggests that the bare working point should be moved so that the stop bands are no longer crossed once the necktie has sufficiently shrunk with increased energy.

3.2.3 *Stop band compensation for $\Delta Q = 0.6$*

Whatever the working area, the stop bands crossing the necktie should be compensated for at best, even dynamically. This is particularly true for the systematic resonance ($3Q_y = 16$) and the quadrupolar resonance ($2Q_y = 9$ or 11). It appeared that the compensation of the second-order resonance was straightforward compared with the compensation of the systematic resonance. As a result of compensation, one could observe that large amplitudes were not lost.

3.2.4 *Filling the aperture*

The obvious way to raise the intensity limit is to increase the beam dimension so that it almost fills the aperture. This is achieved by some injection mis-steering plus excitation of the linear coupling resonance. Thus, the energy from the radial plane is transferred to the vertical plane helping to increase the injection efficiency (more particles avoid the septum) and to create a vertical distribution where large amplitudes dominate.

3.2.5 *Flat bunches (Bf)*

Amongst ideas to improve the bunching factor, the proposal that is used since 1982 consisted in adding a second-harmonic RF system to the fundamental one with careful control of the voltage and the phase between the two cavities. Not only it provides an increase of the bunching factor of 30% by flattening the bunch and thus immediately, 30% more particles can be accommodated in the available tune spread of 0.6, but also a 30% increase of the bucket area, which was welcome at that time.

3.3 *Instabilities*

3.3.1 *Beam loading*

No provisions for any feedback had been made for the fundamental RF system. This inevitably led to problems at beam capture with more than 6×10^{12} protons per ring. A fairly simple fixed frequency feed-forward device active during capture and ejection greatly improved the stability. A fast feedback around the final amplifiers of the second harmonic RF cavities prevented any beam loading effect.

3.3.2 *Longitudinal instabilities*

Longitudinal instabilities were the first to prove troublesome once the PSB had its intensity boost when going to the high working point region. These were coupled bunch mode instabilities (even if they were not identified as such at that time). All of the longitudinal modes from quadrupoles to octupoles could be cured by a feedback system with 15 kHz bandwidth, which was necessary to accelerate more than 2.5×10^{12} protons per ring. This has stimulated a number of similar systems in other machines. Since the PSB has been modified for LHC with fundamental harmonics $h = 1$ or 2, these coupled bunch instabilities did not occur ($h = 1$) or have not been observed ($h = 2$).

3.3.3 *Transverse instabilities*

Transverse instabilities have never constituted a major problem, as the octupole excitation programme provided sufficient Landau damping to keep the beam stable; any intensity gain is accompanied with emittance increase and more space-charge tune spread. Nevertheless a Transverse Feedback System was built which, when properly tuned, gave a 2% to 3% intensity increase and a reduction in the vertical emittance.

3.4 **Extraction**

3.4.1 *From 800 MeV to 1 GeV*

To improve the antiproton production during the AC era, the number of particles accelerated through the PS had to be increased. To overcome the PS space-charge limit, the PSB extraction energy was increased to 1 GeV, decreasing the tune spreads by 1.27 and the beam emittance in the transfer line by 1.15. As a spin-off a new record of particles accelerated in the SPS was observed with reduced beam losses in the PSB-PS transfer line.

3.4.2 *From 1 GeV to 1.4 GeV*

Again, with the unprecedented beam brightness required for the LHC and to help the PS to cope with space charge at low energy, the extracted energy of the PSB was increased to 1.4 GeV (see below).

3.4.3 *Recombination*

Over time, many ways to recombine the bunches from the four rings were used. Since the beginning the four rings are extracted one after the other (order 3, 4, 2, 1) to form a chain filling the whole PS circumference; for the antiproton production, two rings were ejected at the same time and added vertically with a 1 mm double septum, yielding 10 bunches with a doubled line density (1.7 experimentally) at the expense of the vertical emittance increased by a factor of three; for the AC era, two consecutive PSB bunches, each slightly less than 180° long, were merged into a stationary PS bucket, the vertical trajectory of bunches from two different rings being adjusted by a square-wave vertical deflector leading to a vertical emittance only blown-up by a factor 1.5; for ISOLDE, the bunches from different rings can be staggered in time (from 0 to 15 μ s) to cope with the physics needs; for the LHC, six bunches ($h = 1$) from the rings are extracted to fill six PS stationary buckets at $h = 7$ (a first batch of four, then a second one of two bunches); when possible in terms of intensity and emittances, only one three-ring batch is sent from the PSB (two bunches/ring with RF voltage at $h = 1$ to have the right time distance between two consecutive bunches) to fill the six out of seven PS stationary buckets.

3.5 **Big Bang for the LHC**

For the LHC era and to cope with the high-brightness and high-space-charge beams in the PSB and in the PS, many improvements had to be made without the possibility of reversal: to fill the PS with a

single PSB batch would have required an intensity in the PSB such that at injection energy the incoherent tune shift would be as high as $\Delta Q \sim 1$. This is reduced to a more tolerable ~ 0.5 with two batches coming from the PSB. This two-batch filling (one half of the PS per batch) is only possible with one bunch per PSB ring, thus the PSB–RF system had to be changed from $h = 5 + 10$ to $h = 1 + 2$. The first batch is waiting for 1.2 s on the PS injection front porch until the second batch arrives. At 1 GeV, an incoherent space-charge tune shift of ~ 0.3 leads to excessive transverse emittance growth during storage, at least for the “ultimate” beam (LHC “beam–beam limit”). At 1.4 GeV, ΔQ drops by ~ 0.2 owing to $1/\beta\gamma^2$ scaling, and no blow-up was observed. This was also possible as no sign of magnet saturation of the PSB magnet was observed, at least for ring 3. A lot of modifications were needed for the upgrade: renewal of the whole main power supply; reinforced water cooling for the PSB; new $h = 1$ and recycled $h = 5$ to $h = 2$ RF systems, all equipped with fast feedback drivers; transfer kickers for 1.4 GeV; new transfer septa and their capacitor discharge power supplies; change of the transfer line magnets to laminated ones and of their power supplies to cope with the different extraction energies and/or the new currents.

These modifications were undertaken during a shutdown and were finally successful, despite the need for a trim power supply to be added to power the external gaps of the main magnet. Owing to their construction, these gaps are more affected by the iron saturation and 70 G/8000 G were lost. Fortunately the PSB constructors had the good idea to build the magnet such that outer rings can be powered “independently” from the inner rings. We are grateful to them.

4 The future

Obviously, the intensity in the PSB is limited by the tune shift at the injection energy of 50 MeV [21]. To ease the production of the ultimate beam for the LHC, to prepare for the LHC upgrade and to fill experiments with more intensity, CERN is constructing a new linear accelerator (Linac 4). It will provide H^- injection at 160 MeV, thus increasing $\beta\gamma^2$ by a factor of two, allowing a potential factor of two of beam brightness, or possibly a factor of two in beam intensity. In addition, the charge exchange injection can provide a $\sim 10\%$ improvement in the transverse and longitudinal distributions to further reduce the tune shift. As usual, an increase of beam intensity or density will probably generate instabilities. This point is currently being studied in the PSB.

5 Conclusions

From this review, it is obvious that this machine was built to accelerate high beam density and intensity. Not only it surpasses the original goal by a factor of four, but also it allowed an increase in the extracted energy from 0.8 GeV to 1.4 GeV (a factor of 1.46 in magnetic field) without loss of efficiency, extraction of the beam from the four rings in different ways to satisfy the physics request and the generation of beams from 2×10^9 to 10^{13} particles (a factor of 5000 in dynamic range) per ring.

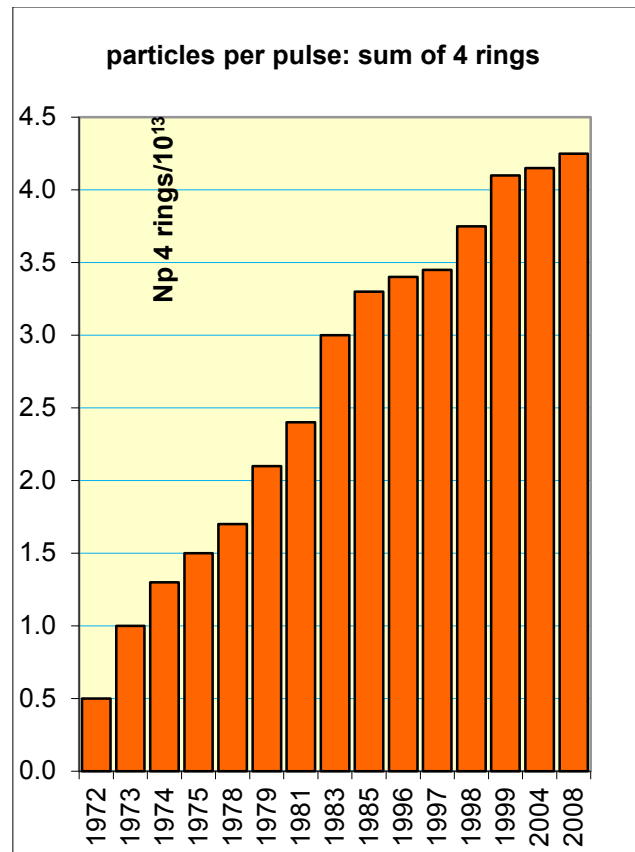


Fig. 1: Evolution of the PSB intensity over the years

The machine proved to be so versatile that it also accelerated ions from deuterons to lead without any major problems. It is now prepared for the next challenge: to inject and accelerate the protons from the Linac 4 at unprecedented intensity and density.

Long live the PSB!

References

- [1] CERN Courier, Vol.37, No.6, July/August 1997, pp. 3-4.
- [2] C. Bovet and K.H. Reich, A four-ring vertically stacked 800 MeV booster injector for the CERN Proton Synchrotron, Proc. 1967 Cambridge Accelerator Conf., 11–15 September 1967.
- [3] K.H. Reich, The PSB seen as a Particle Accelerator, SI/Note DL/73-2.
- [4] K.H. Reich, The CERN PS Booster, a flexible and reliable injector, CERN/PS/BR 76-14 (1976) and V all-Union National Conf. on Particle Accelerators, Dubna, 5–7 October 1976.
- [5] K. Schindl and the PSB Staff, *IEEE Trans. Nucl. Sci.* **NS-28** (1981) 2803.
- [6] B.W. Allardyce *et al.*, ISOLDE: a new client for the CERN PS Booster, Proc. Second European Particle Accelerator Conf., Nice, France, 12–16 June 1990.
- [7] B.W. Allardyce *et al.*, ISOLDE at the PS Booster, Proc. Third European Particle Accelerator Conf., Berlin, Germany, 24–28 March 1992.
- [8] A. Blas *et al.*, Beams in the CERN PS complex after the RF upgrades for LHC, Proc. Sixth European Particle Accelerator Conf., Stockholm, Sweden, 22–26 June 1998.

- [9] A. Blas *et al.*, Conversion of the PS Complex as LHC Proton Pre-Injector, Proc. 1997 Particle Accelerator Conf., Vancouver, Canada, 12–16 May 1997.
- [10] M. Benedikt (Ed.) *et al.*, The PS Complex as Proton Pre-Injector for the LHC: Design and Implementation Report, CERN 2000-003 (2000).
- [11] M. Benedikt, M. Chanel and K. Hanke, Performance of nominal and ultimate LHC beams in the CERN PS-Booster, Proc. Tenth European Particle Accelerator Conf., Edinburgh, UK, 26–30 June 2006.
- [12] K.H. Reich, Some reflexions on the CPS Booster, MPS/Int. DL/B 66-5.
- [13] C. Bovet and K.H. Reich, Nominal values of Q_h and Q_v for the Booster and their range of tuning, SI/Note DL/68-4.
- [14] U. Bigliani *et al.*, Influence on the beam intensity on the design of the CERN PS Booster, Proc. 7th Int. Conf. on High Energy Accelerator, Yerevan, 1969.
- [15] K.H. Reich, The CERN Proton Synchrotron Booster, Proc. 1969 Particle Accelerator Conf., Washington, DC, 5–7 March 1969.
- [16] K.H. Reich, Optimisation of the Overall Design of a Synchrotron, SI/Note DL/71-1.
- [17] H. Koziol *et al.*, Results from the running-in of the CERN 800 MeV Booster, CERN/MPS-SI/Int. BR/72-4.
- [18] J. Gareyte *et al.*, *IEEE Trans. Nucl. Sci.* **NS-22** (1975) 1855.
- [19] G. Gelato, L. Magnani, N. Rasmussen, K. Schindl and H. Schonauer, Progress in space-charge limited machines: four times the design intensity in the CERN Proton Synchrotron Booster, Proc. 1987 Particle Accelerator Conf., Washington, DC, 16–19 March 1987.
- [20] R. Cappi *et al.*, Upgrading the CERN PS Booster to 1 GeV for improved antiproton production, Proc. 1989 Particle Accelerator Conf., Chicago, IL, 20–23 March 1989.
- [21] M. Chanel, Space-charge measurement at the PSB, Proc. Beam07, CERN, Geneva, 1–5 October 2007.

Linac 2

1 Introduction

The commissioning of the Proton Synchrotron Booster (PSB) in 1972 shed light on the inherent limitations of Linac 1 as an injector for the newly built synchrotron. Whereas injection from Linac 1 to the Proton Synchrotron (PS) was single-turn, the multiturn injection introduced with the PSB had been designed for long linear accelerator (linac) pulses, up to 100 μs , and high beam current, 100 mA. Although the Linac 1 upgrade program launched in parallel with the construction of the PSB succeeded in increasing the pulse length to 80 μs and the beam current to 50 mA, at the limit of what was achievable by the Linac 1 radiofrequency (RF) and focusing systems, these values were still far from what the PSB was ready to accept. Moreover, because of their relatively old design, the vacuum and RF systems of Linac 1 required a lot of attention and were a continuous cause of beam down time. The impressive progress in linac and vacuum technology realized in the 1950s and 1960s suggested that a new linac could have improved not only the performance but also the availability of the PSB and PS injector [1].

The decision to build a new linac injector, at the 50 MeV energy of the PSB injection, was therefore taken in October 1973. The design parameters were chosen in order to comfortably exceed the nominal PSB requirements, providing a safety margin during operation and for future upgrades. The beam current was specified as variable between 50 mA and 150 mA, for a maximum pulse length of 200 μs . The design repetition frequency of 2 Hz was also intended to accommodate future upgrades of PSB and PS from the standard 1.1 Hz. The decision was taken to install the new linac in a new building parallel to the Linac 1 location instead of in the Linac 1 tunnel, in order to avoid a long shut-down for installation and commissioning and to have Linac 1 available as a back-up during the first years of operation of Linac 2.

Construction of the “new linac”, later called “Linac 2”, started in December 1973, and the first 50 MeV beam was obtained on 6 September 1978. Only a month later the design current was reached and the first injection tests in the PSB started. Routine operation for the PSB started soon after, in December 1978. As proudly announced at the time, Linac 2 was completed “on budget and on schedule”, for an overall cost of 23 million CHF at the time [2].

2 Machine layout

The proton beam is generated by a duoplasmatron ion source, which can provide a current of up to 300 mA. In the original configuration, a Cockcroft–Walton generator at 750 kV located in a shielded room separate from the accelerator hall (Fig. 1) provided the pre-acceleration to the entrance of the Low Energy Beam Transport (LEBT). The 5.66 m long LEBT contained 18 quadrupoles, a complete emittance measurement device together with other diagnostics and a bunching system made of three RF cavities, two at the basic frequency of 202.56 MHz and one at double harmonic frequency.

The main accelerator is a Drift Tube Linac (DTL) of standard Alvarez design, presenting many improvements with respect to the Linac 1 design. The three accelerating tanks, accelerating the beam up to 10.3 MeV, 30.5 MeV and 50 MeV, respectively, have in common the RF frequency (202.56 MHz) and the vacuum envelope. The drift tubes are suspended from a girder; they are aligned externally and successively introduced into the tanks. A mechanical positioning system on the outside of the girder together with a bellow on the inside allows positioning of the drift tubes with the required precision. The tanks are made of mild steel co-laminated with a copper sheet. Vacuum and RF tightness are provided by aluminium wire joints. Post-couplers provide stabilization of the RF field against mechanical imperfections. The three tanks have a total length of 33.3 m [3, 4].



Fig. 1: Linac 2 750 kV Cockcroft-Walton generator, source and accelerating column



Fig. 2: Linac 2 tanks

Beam optics requirements for the new linac were particularly demanding because of the high space charge forces related to the 150 mA current, in particular in the LEBT and in the first Alvarez tank. Focusing is provided by pulsed electromagnetic quadrupoles placed inside the drift tubes and in the low- and high-energy transport lines. A careful six-dimensional emittance matching between the different linac sections was achieved thanks to an extensive use of modern (for the 1970s) beam simulation codes. Owing to the strong space charge, a transverse emittance increase by a factor of 2.5

was measured inside the linac; however, the output emittance of 15π mm mrad (90% of the beam) is still a factor of two smaller than the PSB acceptance [2, 5].

The RF system incorporated, as main high-power stages, an improved version of the Linac 1 units, with larger diameters in order to safely deliver more RF power, and improved insulators, neutralization and electronics. The RF tube was the same triode (TH170R) already used for most of the Linac 1 chains. In this configuration, the final amplifiers used for the linac tanks were able to reach a peak power of 2.5 MW. Rigid coaxial lines equipped with motorized trombones then transport this power to the cavities, through an adjustable power loop designed to cope with a large range of beam currents. New low- and medium-power amplifiers were developed as driving stages for the Linac 2 amplifier chains, allowing a modular construction of the different RF chains also covering the buncher and debuncher amplifiers. The 40 kV anode supply for the final stages is provided by a large pulse-forming network (PFN) circuit. The important beam loading due to the high linac current could be mastered thanks to a newly developed fast feedback electronics, which can provide up to 1% and 1° stability in voltage and phase in the tanks, respectively [6].

At the exit of the accelerating tank, a line transports the beam up to the connection point with the Linac 1 to PSB line. Initially, the line was equipped with three debunching cavities (one at double harmonic), later reduced to one because of the larger than foreseen longitudinal emittance. Single-pulse transverse and longitudinal emittance measurement lines were installed immediately at the exit of the linac, to complement the existing “old measurement lines” at the PSB entrance. A full longitudinal emittance measurement could be performed using a dedicated bunch rotating cavity in the measurement line.

3 Improvements

A major improvement to Linac 2 was the replacement of the 750 kV Cockcroft–Walton generator and of the old LEBT with a new Radiofrequency Quadrupole (RFQ) together with a new source and new low- and medium-energy beam transports, which took place during the 1992/93 shut-down.

After the successful construction of a prototype RFQ for Linac 1, the development of a high-intensity RFQ for Linac 2, capable of delivering to the Alvarez DTL a current of 200 mA, started already in 1984. A first high-current RFQ was commissioned on a test stand in 1989, and following this successful test the replacement of the Linac 2 pre-injector was officially approved in 1990 [7]. The main motivation for the higher current was related to the preparation of the CERN injectors for the Large Hadron Collider (LHC) that was starting in these years. It was clear that LHC would require unprecedented beam brightness (current over-emittance) from the injector chain, and one of the options considered was to go to single-turn injection into the PSB of a high-current linac beam, to minimize emittance growth. This in turn required the highest achievable current from the linac; simulations showed that in spite of the fact that the 200 mA beam from the RFQ was strongly mismatched longitudinally in the first DTL tank, which had been designed for 150 mA, a maximum current of 180 mA (within the required emittances) was achievable at the exit of the linac. Of course, another motivation for the replacement was the simpler operation and maintenance with the smaller RFQ as compared with the large Cockcroft–Walton installation.

Construction of the new RFQ started soon after approval, and the new system, called RFQ2, was installed at Linac 2 at the place of the old LEBT during the normal shut-down 1992/93. Commissioning of the RFQ2 with Linac 2 took a few weeks, and the 1993 physics run started with the new RFQ injector.

The RFQ2 system consists of a new duoplasmatron proton source (see Fig. 3) with a 90 kV extraction, followed by a short two-solenoid LEBT of less than 1 m [8]. The four-vane RFQ (RFQ2) of 1.8 m length was entirely built at CERN and operates at the record voltage of 178 kV,

corresponding to 2.4 times the Kilpatrick limit. The high vane voltage is required by the large space charge of the 200 mA beam, so far the highest intensity reached by an operational RFQ. Longitudinal matching to the Alvarez DTL is performed by two bunching cavities. Figure 4 shows the RFQ as installed in front of the Linac 2 tanks.



Fig. 3: The Linac 2 duoplasmatron proton source



Fig. 4: RFQ2 and Linac 2 tanks

During the first years after installation, the RFQ was operated at voltages slightly below nominal in order to limit RF breakdowns to levels compatible with the reliability required for the CERN injector. This in turn limited the beam current from the RFQ to values of around 180 mA. The progressive upgrade and cleaning of the vacuum system allowed the design voltage to be reached a

few years after installation, with the RFQ delivering beam currents in excess of 200 mA, which corresponded to currents in excess of 180 mA at the exit of the linac.

The transverse beam optics of the Alvarez DTL has remained largely unchanged since the RFQ was installed. However, the approximately 100 m long transfer line to the PSB has had major optics changed, once to convert to a more ordered FODO structure, and a second modification to cancel the dispersion at the entrance of the PSB [9].

Other improvements to Linac 2 after construction were mainly aimed at keeping the required reliability and to adapt to the evolving technologies. These included the commissioning of a new control system in 1993, the installation of new low-power solid-state amplifiers and the replacement of the interlocks and of the electronics of the high-power amplifiers on the RF systems. In the last 5 years, approximately half of the quadrupole magnet power convertors have been modernized, as well as the vacuum control system.

4 Conclusions

It was the rapid progress in linac technology that made possible the replacement of Linac 1 after 20 years of operation with the new Linac 2, providing a factor of two increase in both current and pulse length, with the additional advantages of increased reliability and reduced maintenance.

Even nearing the end of its life, Linac 2 still has a remarkable reliability record. In the period from 2006 to 2009, it averaged 97.5% availability, with almost half of its down-time being attributed to external factors (i.e. power cuts or cooling water stops).

In the same way Linac 2 has now been operating smoothly and reliably for more than 30 years, but now shows similar limitations to those that led to the replacement of Linac 1. On the one hand, the exploration of possible options for a LHC luminosity upgrade indicates that the first bottleneck for achieving a higher intensity in the PS complex is the PSB injection, where the space charge tune shift at 50 MeV limits the total intensity. The only way to go beyond this limitation is by increasing the linac energy, which in turn requires the construction of a new linac, an appreciable energy increase of Linac 2 being prevented by the lack of space at the end of the linac. On the other hand, in recent years Linac 2 has developed serious vacuum problems due to its now “old-fashioned” construction technology, which constitute a serious threat for operation. Moreover, procurements of the RF tubes, whose design dates basically to Linac 1, is becoming more and more difficult, and there are concerns that they could be unavailable in the future.

These considerations suggest that the times are mature for the replacement of Linac 2 with a new linac, which would also profit from recent advances in linac technology such as acceleration of low-current long-pulse H^- beams, chopping at low energy for minimum beam loss and modern beam dynamics design. Considering all of these arguments, the CERN management has approved in June 2007 the construction of the 160 MeV Linac 4, which will be placed in a new building, parallel to the present Linac 2 location. The project has started in 2008, and connection of the new linac to the PSB is foreseen for 2015.

References

- [1] D.J. Warner (ed.), Project Study for a new 50 MeV Linear Accelerator for the C.P.S., CERN/MPS/LINP 73-1 (1973).
- [2] E. Boltezar *et al.*, The new CERN 50-MeV Linac, Proc. 1979 Linear Accelerator Conf., Montauk, NY, 10–14 September 1979.

- [3] D. Warner, Accelerating structures of the CERN new 50 MeV linac, Proc. 1979 Linear Accelerator Conf., Montauk, NY, 10–14 September 1979.
- [4] E. Boltezar, Mechanical design of CERN new linac accelerating structures, Proc. 1979 Linear Accelerator Conf., Montauk, NY, 10–14 September 1979.
- [5] D.J. Warner and M. Weiss, Beam optics in the CERN new 50 MeV linac, Proc. 1979 Linear Accelerator Conf., Montauk, NY, 10–14 September 1979.
- [6] J. Cuperus, F. James and W. Pirkel, The RF system of the CERN “New Linac”, Proc. 1979 Linear Accelerator Conf., Montauk, NY, 10–14 September 1979.
- [7] J.L. Vallet, M. Vretenar and M. Weiss, Field adjustment, tuning, and beam analysis of the high-intensity CERN RFQ, Proc. Second European Particle Accelerator Conf., Nice, France, 12–16 June 1990.
- [8] M. Weiss, The RFQ2 complex: the future injector to CERN Linac 2, Proc. Third European Particle Accelerator Conf., Berlin, Germany, 24–28 March 1992.
- [9] K. Hanke, J. Sanchez-Conejo and R. Scrivens, Dispersion matching of a space charge dominated beam at injection into the CERN PS booster, Proc. 2005 Particle Accelerator Conf., Knoxville, TN, 16–20 May 2005.

The Antiproton Accumulator, Collector and Decelerator Rings

1 Introduction

Proton–antiproton colliders were first discussed at CERN in 1962, 7 years after the discovery of the antiproton at the Bevatron in Berkeley. Considerations included the Intersecting Storage Rings (ISR), then in their early design stage. It was concluded in 1962 that with the expected densities of antiproton beams, luminosities were discouragingly low. However, prospects changed in 1966, with Budker's and O'Neill's [1, 2] ideas of electron cooling. In Ref. [2], Budker describes the application of his invention specifically for the accumulation of antiproton beams dense enough to make proton–antiproton colliders viable. These need only a single ring, a concept already practised at that time with electron–positron colliders. Rubbia, realizing the potential offered by the projected “300 GeV Machine” later built at CERN as the Super Proton Synchrotron (SPS), proposed, still in 1966, to use it as a proton–antiproton collider.

The next step occurred in 1968, when van der Meer invented stochastic cooling (published only in 1972, see Ref. [3]). Both electron and stochastic cooling were experimentally proven in 1974, at the NAP-M storage ring in Novosibirsk [4] and at the CERN ISR [5], respectively. With these tools at hand, Rubbia *et al.* [6] revived the idea of converting the SPS into a proton–antiproton collider, with the specific aim of producing the long-awaited W and Z bosons. At that stage, Rubbia *et al.*'s scheme was still based on electron cooling.

The following stride was the Initial Cooling Experiment (ICE) [7], a 2 GeV storage ring to test electron and stochastic cooling. It was quickly built during 1977, using the magnets of the g-2 ring, previously employed to measure the magnetic moment of the muon. Early in 1978, stochastic cooling proved so successful (Fig. 1) that the collider scheme was then entirely based on it. Already in 1976, Strolin *et al.* [8] had proposed an accumulator ring using stochastic cooling, to provide dense antiproton beams for the ISR.

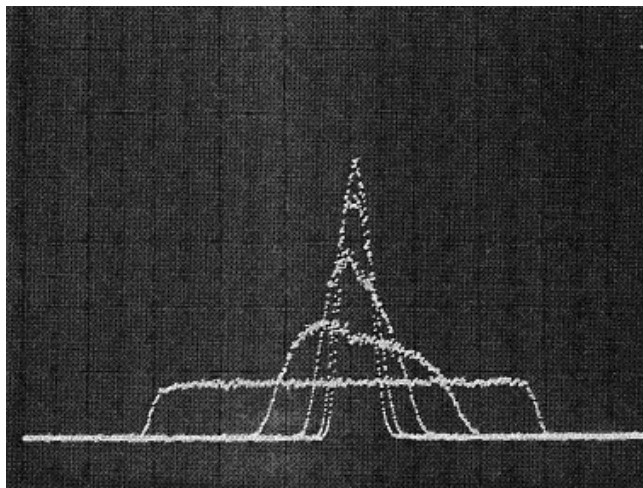


Fig. 1: Demonstration of stochastic momentum cooling in ICE. The momentum distribution of 5×10^7 circulating protons was first spread out by applying noise around a harmonic of the revolution frequency on a radiofrequency (RF) cavity (first Schottky scan, rectangular shape). Then cooling was turned on. Scans at 1 minute intervals show the concentration of the protons with initially $\Delta p/p = \pm 3 \times 10^{-3}$ into a narrow momentum bite of $\pm 0.5 \times 10^{-3}$. The signal height is proportional to the square root of the particle density, and the abscissa is $\Delta p/p$.

Stochastic cooling in ICE, apart from increasing the density of the beam, extended its lifetime, given by Coulomb scattering on the residual gas, from hours to days. This permitted a test of the

lifetime of the antiproton [9], the first particle physics experiment performed with the aid of stochastic cooling: CPT stipulates identical decay lifetimes for antiprotons and protons, practically infinite compared with the required days of accumulation time. Prior to ICE, the experimentally lower limit for antiprotons was only 120 μs (derived from bubble chamber tracks). Despite faith in theory, it was a nightmare to launch a multimillion-dollar project in such a situation. To remove doubts, a crude antiproton production target was inserted into the transfer line between PS and ICE, which converted 10 GeV/c protons (the maximum momentum transferable in the line) to 2 GeV/c antiprotons (the maximum storable in ICE). In this way a beam of 240 antiprotons could be stored and was stochastically cooled in ICE. Four days later, 80 were still circulating. This established a new lower limit for the decay lifetime of 32 h at rest, an improvement by 9 orders of magnitude and a relief for those who needed more than just faith in CPT.

The results from ICE led to a rapid decision to go ahead with the construction of the Antiproton Accumulator (AA) based on stochastic cooling. The antiprotons were cooled and accumulated directly at 3.5 GeV/c [10, 11], where the yield from 26 GeV/c (PS) protons is highest. The overall scheme (Fig. 2) also involved major modifications to the PS.

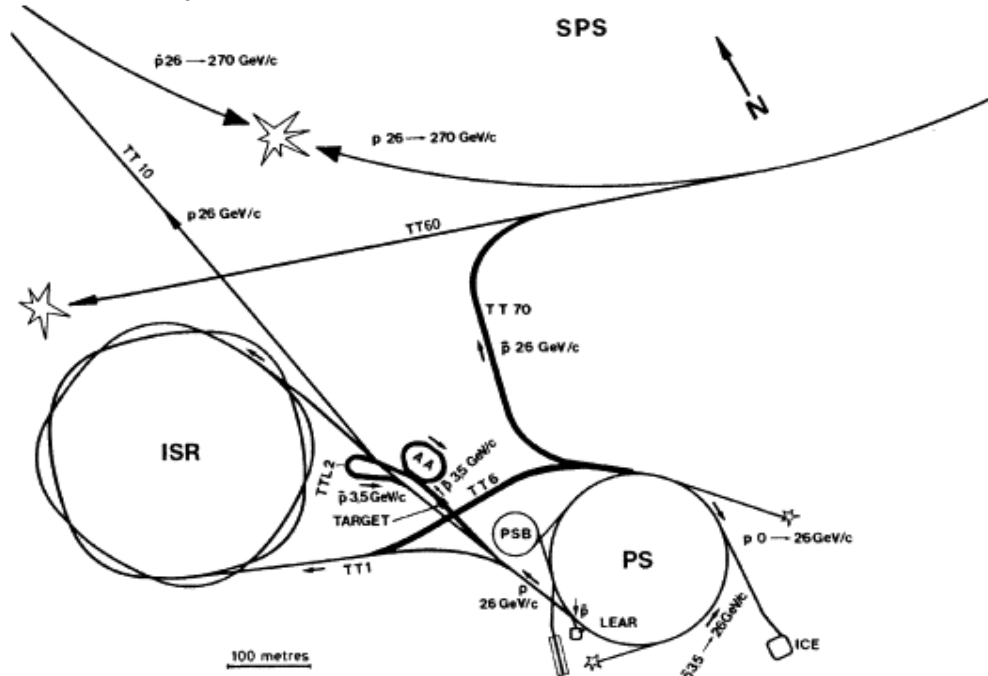


Fig. 2: Layout of the CERN accelerators in 1981. LEAR, still under construction in 1981, is also shown

Construction of the AA began in 1979. In April 1981, the first proton–antiproton collisions occurred in the ISR, at 2×25 GeV. The SPS followed on the heels, with collisions at 2×273 GeV on 10 July 1981. The first W data were taken in 1982 and the discovery of the W and Z was announced in 1983. In order to satisfy the ever-increasing appetite of antiproton users, the Antiproton Collector (AC) [12] was built around the AA in 1986. From 1987 on, it boosted the accumulation rate, eventually by an order of magnitude. After a last collider run in 1991, the SPS returned to an accelerator-only life. The Low Energy Antiproton Ring (LEAR) continued to take beam from the AC/AA until end 1996. In 1997, the AA was dismantled and the AC converted into the Antiproton Decelerator (AD), to provide low-energy antiprotons in a simpler way [13].

2 Outline of the scheme

The 50 MeV Linac, the 800 MeV Booster and the 25 GeV PS (Fig. 2) were pushed hard to deliver an intense proton beam on the production target. The burst of antiprotons emerging around 3.5 GeV/c

was captured in the AA (or, after 1987, in the AC). In the original AA, a fresh burst of antiprotons remained on the injection orbit for at least 2.4 s for stochastic pre-cooling of the momentum spread. The RF system then trapped and moved them to the stacking region where stack-tail cooling took over. The injection region was now free for the next burst of antiprotons, arriving 2.4 or 4.8 s later. This sequence was repeated during the whole accumulation period (Fig. 3).

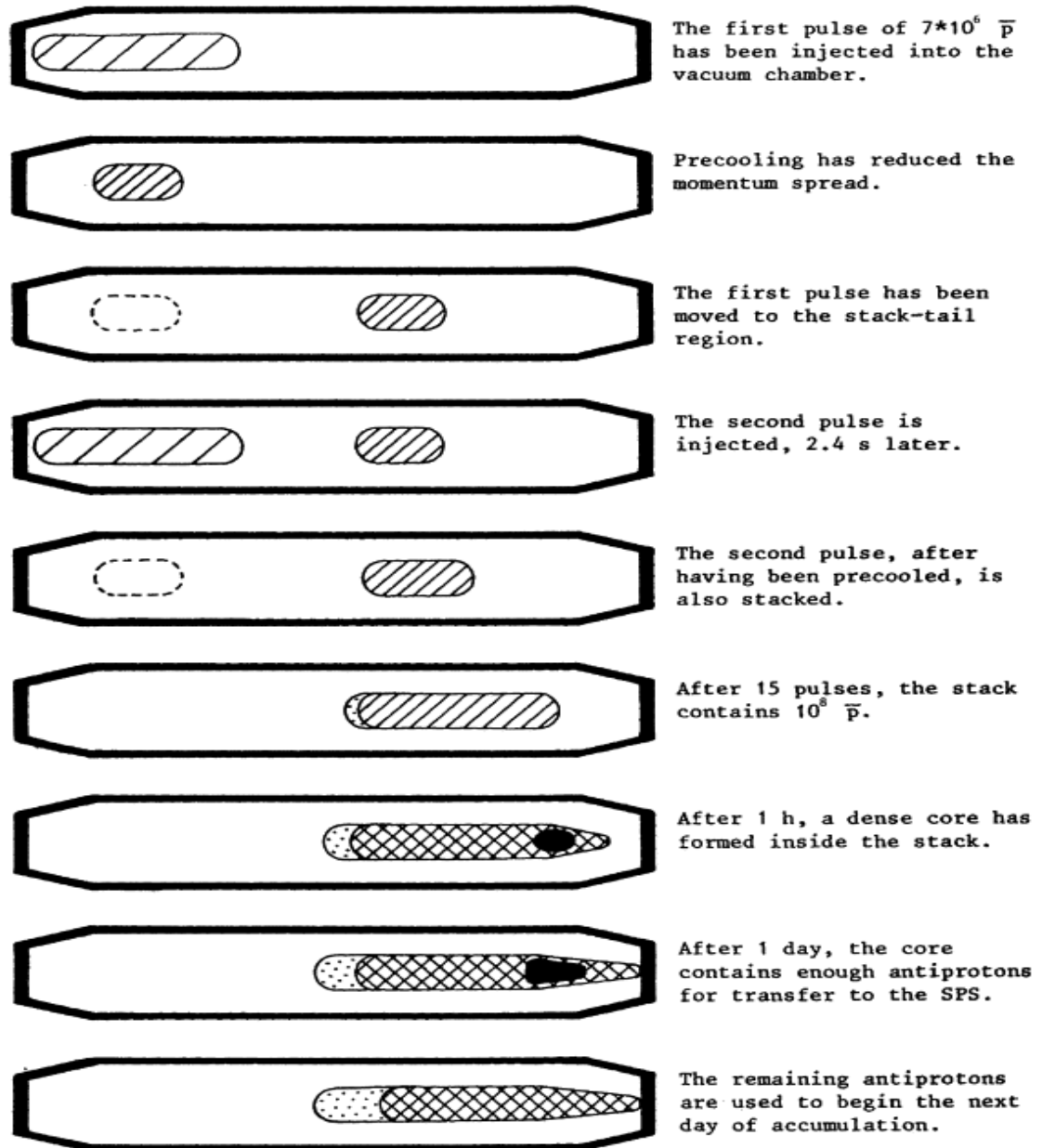


Fig. 3: Schematic sequence of injection, cooling and accumulation in the original Antiproton Accumulator, before the advent of the Collector. (Reproduced with permission from Ref. [11]).

In the AC, a powerful “bunch rotation” RF system (1.5 MV, 9.5 MHz) turned the incoming five antiproton bunches into a nearly continuous beam of lesser momentum spread. Stochastic cooling in all three planes then reduced the emittances by large factors. Another RF system (3.5 kV, 1.6 MHz) re-bunched the antiprotons, for ejection and transfer into a matched bucket on the AA injection orbit.

Both in the original and the modified AA, the antiproton stack was subjected continuously to up to six different stochastic cooling systems. Over a day, a stack with a dense core of several 10^{11}

antiprotons was accumulated. An antiproton bunch was picked from the stack by creating an “unstacking bucket” in the core region and moved to the ejection orbit. From there it was sent through a “loop” (TTL2, Fig. 2) to the PS. For use in the Collider it was accelerated to 26 GeV/c and sent to the SPS as described in Section 3.1.3 below. Prior to a transfer, careful checks were performed, concluded by the dispatch of a small “pilot bunch” of about 10^9 antiprotons all of the way from the AA to the SPS. This assured that the big shot, containing a day's harvest, would safely find its way. Transfers of antiprotons to LEAR were made in a different way, described in Ref. [13].

3 Antiproton production and accumulation

3.1 The role of the PS

3.1.1 *High-intensity primary proton beam*

The production of a large number of antiprotons demands a proton beam of an intensity as high as the target will stand. The transverse emittances have to be small, to permit focusing to a small size over the whole length of the target. Finally, the proton burst length has to correspond to the AA circumference, one quarter that of the PS.

This means that the PS beam, normally 20 bunches around the whole circumference, had to be crowded into 5 bunches. The fact that the 800 MeV PS Booster consists of four superposed rings, each one quarter of the PS circumference, was helpful. The beams from two Booster rings (five bunches each) were ejected simultaneously, combined in the vertical plane, and injected into the PS. This was repeated with the other two rings, timed such that two sets of five bunches circulated on opposite sides of the PS. After acceleration to 26 GeV/c, on the flat top, one set was slightly accelerated and advanced towards the other. When the two sets had fallen into step, they were ejected towards the target. Later, for the AC, different techniques of bunch merging were used, but the goal, to compress the beam into five bunches distributed over one quarter of the PS circumference, remained the same.

Nominally, that process was repeated every 2.4 s, but usually the interval was extended to 3.6 or 4.8 s, in order to give more time to cooling in the AA, and to allow the PS with its basic 2.4 s cycle to serve other users in between. The intensity was raised from a prudent 10^{13} to finally 1.3×10^{13} protons per pulse.

3.1.2 *Post-acceleration of antiprotons*

The momentum of 3.5 GeV/c was too low for direct transfer to the SPS. Therefore, the antiprotons, extracted in single bunches from the AA, were sent to the PS via the newly built “loop” (TTL2, see Fig. 2), for acceleration to 26 GeV/c. Subsequent “bunch rotation” reduced their length to about 4 ns before transfer to the SPS through the new TT70 line (Fig. 2). This process was repeated every 2.4 s, until three (later six) antiproton bunches were circulating on the SPS injection orbit, equidistantly spaced. For a check, the transfer of the same number of “cheap” proton bunches preceded that of the “precious” antiprotons.

3.1.3 *Proton test beams for AA and AC*

Initial setting up of the AA (later also of the AC) was done with protons. For this purpose, the PS produced single bunches at 3.5 GeV/c, which first followed the path of the 26 GeV/c protons towards the target location and then, with the target removed, through the antiproton injection line to the AA (later the AC), which for that purpose had all magnets in “opposite polarity”.

Precision setting up of the AA and AC magnets had to be done in “normal polarity”, and the 3.5 GeV/c proton test beam from the PS came through the loop (TTL2). This was done also during

routine operation, preceding antiproton transfers from the AA to the PS, in order to verify the correct settings of the AA ejection and of the channels.

All of the exercises described above demanded precise tuning of the machines to each other, in terms of magnetic field, orbit position and revolution frequency. Timing logics was intricate, timing precision had to be high, and all of the settings had to be reliably flipped from one operational mode to the other within 1.2 s.

3.2 Antiproton production

Antiprotons are produced by a high-energy proton beam hitting a target. The yield is highest at a momentum corresponding to production at rest in the centre-of-mass system of the incoming protons and the stationary target nucleons [14]. For 26 GeV/c protons, there is a flat maximum around $p \approx 3.5$ GeV/c.

Target material and geometry are chosen to maximize proton interactions, while minimizing antiproton re-absorption. Also, the beam optics before and after the target are vitally important [15, 16]. The rod-shaped target is made of heavy material with a diameter of about 3 mm and a length between 50 and 120 mm (Fig. 4), of the same order as the inelastic collision length. The channel following the target has to match the “antiproton line source” (target) to the acceptance of the ring (AA, later AC). This is obtained by making the horizontal and vertical beta functions at the target approximately equal to its length ($\beta_H \approx \beta_V \approx L_t$). The conversion rate is then (approximately) proportional to $\Delta p \cdot \sqrt{E_H E_V}$ where Δp is the momentum acceptance and $E_V \approx E_H$ the transverse acceptances of the storage ring.

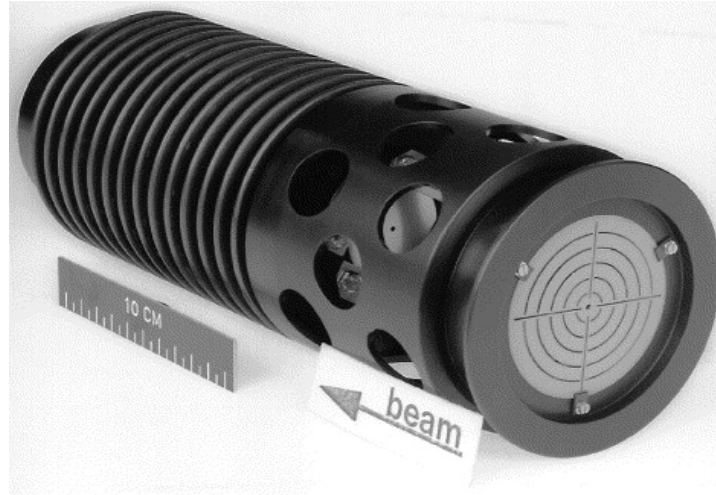


Fig. 4: An antiproton production target for the AA (1980). The tungsten rod is 110 mm long and has cooling fins for forced air cooling. Correct position and size of the 26 GeV/c proton beam from the PS was monitored on a scintillator screen in front of the target, with circles every 5 mm.

For the original AA (in 1984) preceded by a 120 mm long copper target, an antiprotons/protons conversion rate of 0.6×10^{-6} was obtained, with a magnetic horn (Fig. 5) as the collector lens after the target. In the AC, with its larger acceptances, and a 60 mm long iridium target, the best conversion rate was 6×10^{-6} with a lithium lens and 5×10^{-6} with a magnetic horn.

The small-emittance primary beam was matched to the target with quadrupoles and, for a certain period, with an additional lithium lens. For capturing the antiprotons from the target, magnetic horns [17, 18] (Fig. 5), lithium lenses [19, 20] and an experimental plasma lens [21] have been used. Magnetic horns proved more robust and easier to replace in the highly radioactive target area. Lithium lenses gave somewhat better yield. Early operation of the AA was with a horn, then lithium lenses

were used for several years, then there was a return to horns for the late AC period and for the AD.

A magnetic horn is a “current-sheet lens”. Figure 5 shows its principle (a) and a photograph (b) of its inner wall (“horn membrane”). A current flowing through the inner wall and returning via the outer one creates an azimuthal magnetic field in the space between them, but no field inside the horn. Antiprotons produced at large angles traverse the inner wall and are bent towards the axis. The horn membrane had to be thin to avoid scattering and absorption of the penetrating particles. It was made from aluminum, about 1 mm thick. The pulse currents were several hundreds of kiloamperes.

Lithium lenses are rods of lithium, chosen for its low interaction with protons and antiprotons, surrounded by a pulse transformer, which induces a current along the axis. The azimuthal magnetic field inside and outside the rod focuses the particles. Rods of 34 mm diameter were used during SPS Collider operation, while a 20 mm version was designed for operation with LEAR alone. The pulse currents were also several hundreds of kiloamperes.

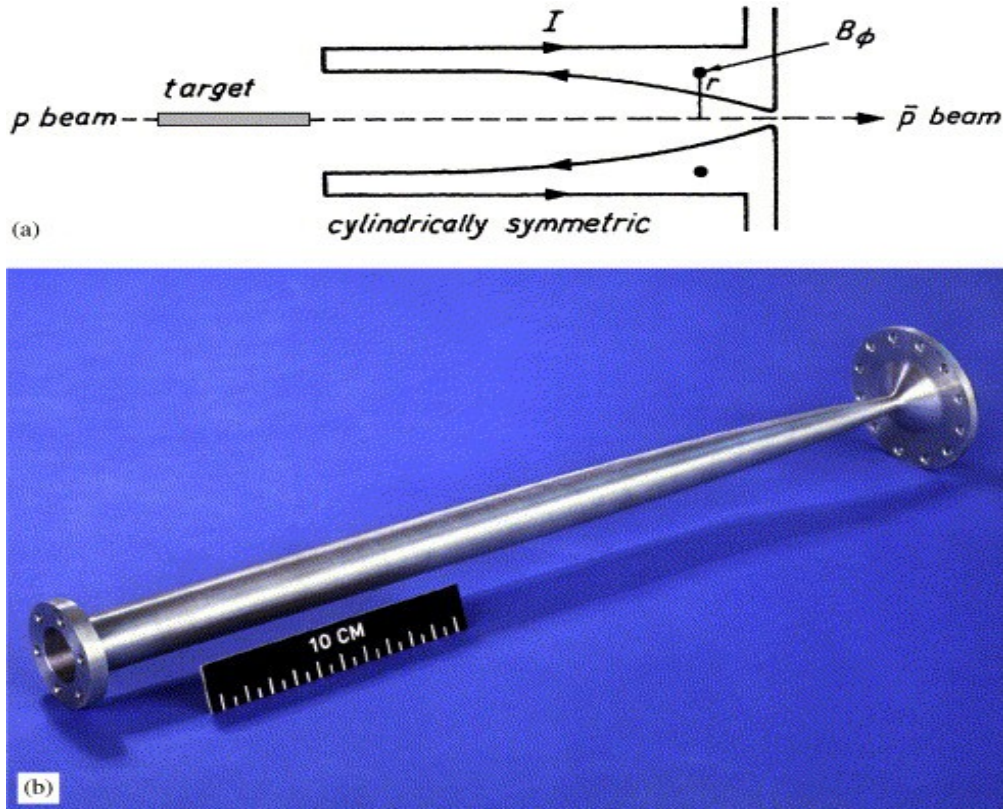


Fig. 5: The magnetic horn of the AA collected antiprotons emitted at large angles from the target: (a) (reproduced with permission from Ref. [11]) the flow of electrical current in a magnetic horn and (b) the inner conductor. The horn was pulsed at 400 kA for 15 μ s (half-sine).

3.3 The AA and AC storage rings

The AA [10, 11, 22] had a circumference of 157 m (Fig. 6). Its magnetic field was constant, for a beam momentum of 3.5 GeV/c on central orbit. It was built in a new hall and later buried under concrete shielding blocks.

The optical properties were quite particular, dictated by the large acceptances required for antiproton collection and the needs of stochastic cooling and stacking. This leads to an impressively wide horizontal aperture, as much as 0.7 m in the regions of large dispersion where the orbit position dependence on the momentum is the strongest, providing spatial separation between the stack and the newly injected beam.

Quadrupoles and bending magnets (weighing 11 and 75 t, respectively) were large in those regions, but of conventional size in the less dispersive regions. Sections with vanishingly small dispersion were required for the location of kickers for momentum cooling of the stack, to avoid “heating” of the horizontal emittance. The injection kicker and the pre-cooling devices had shutters for electromagnetic separation from the stack. An ultra-high vacuum (10^{-11} Torr) assured long storage times and, together with an elaborate clearing system, helped to reduce beam instability caused by ions trapped in the antiproton beam.

The AC, with a circumference of 187 m (Fig. 7), was built in 1986/87 around the AA [22, 23]. Its primary task was to capture an order of magnitude more antiprotons than the AA, for which it had much larger acceptances (Table 1), both transverse and in momentum.



Fig. 6: The AA in its hall, before it disappeared from view under heavy concrete shielding

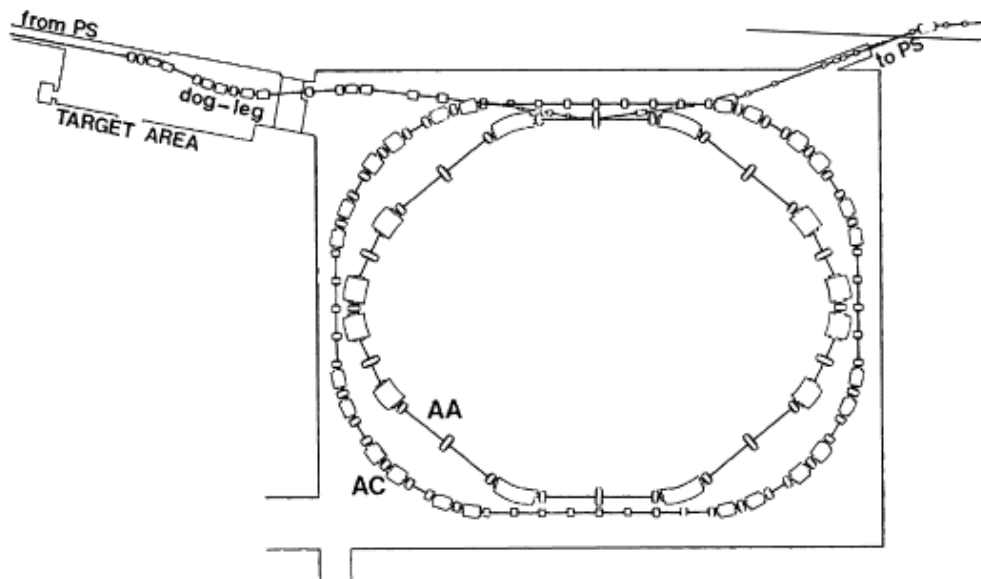


Fig. 7: In 1986/87, the AC was built around the AA and a “dog-leg” incorporated into the injection line to diminish the flux of electrons and π^- reaching the hall (reproduced with permission from Ref. [11]).

A very strong focusing lattice was needed to provide such a large acceptance within an aperture not exceeding 0.35 m. The AC also had regions with strong dispersion and others with zero dispersion, required by stochastic cooling, but in a less extreme way than the AA.

Two large and powerful cavities (each 2 m long and 2.5 m in diameter; together 1.5 MV at 9.5 MHz) were installed in a dispersion-free straight section. After injection they “rotated” the bunches in longitudinal phase space, extending their length and reducing the momentum spread.

Table 1: Acceptances of AA and AC (attained simultaneously)

| Machine | Horizontal E_H (π mm mrad) | Vertical E_V (π mm mrad) | Momentum $\Delta p/p$ (%) |
|---------|-----------------------------------|---------------------------------|---------------------------|
| AA | 85 | 85 | ± 0.75 |
| AC | 200 | 200 | ± 3.00 |

In the AC, a vacuum of a 10^{-8} Torr was sufficient to avoid blow-up due to scattering as well as ion trapping by the low-intensity antiproton beam during the few seconds that the beam stayed in this machine. In the modified AA, the higher intensity and density made an efficient control of beam instability compulsory. Additional clearing by “beam shaking” and active damping of coherent instabilities were vital to reach the new design performance.

3.4 Stochastic cooling and stacking

The AA, and later also the AC, had large numbers of stochastic cooling systems: seven in the original AA, five in the modified AA and nine in the AC. As each of them had to be optimized for a specific task, their characteristics (pickup/kicker technology, bandwidth, gain, power, etc.) differed vastly.

The pre-cooling systems, acting on newly injected beams (less than 10^8 antiprotons), with time constants of a second, needed high-gain, high-power amplifiers. In the original AA, pre-cooling acted only on momentum spread, using Thorndahl's notch-filter method [24]. Pickups and kickers consisted of short ferrite frames around the beam, resembling beam current transformers. Signals were coupled out or in, via one-turn loops on one side of the frame, the opposite side being movable, acting as a shutter. The shutters were opened when the beam was moved out the pre-cooling region. A 2 m long tank contained 100 frames, and there were two kicker tanks and two pickup tanks. The bandwidth was 150–500 MHz, and the amplifier rating 5 kW.

In the AC, pre-cooling was applied in all three phase planes. Pickups and kickers consisted of loop couplers, with electrodes left and right, or above and below the beam. The difference signal served for transverse cooling and the sum signal for momentum cooling. Two plate pairs connected in series formed a “superelectrode”; 24–48 of these (depending on their frequency band) were housed in 2 m long tanks. The electrodes moved in, to follow the shrinking beam size during cooling, thus maximizing pickup sensitivity and minimizing kicker power. The low-level components (pickups, terminations, preamplifiers) were cryogenically cooled to reduce noise. Three bands (1 GHz to 1.65 GHz, 1.65 GHz to 2.4 GHz and 2.4 GHz to 3 GHz) were used, with three combined horizontal/momentum and three vertical/momentum systems, a total of six pickup and six kicker tanks. Amplifier ratings were 4.5 kW for the lower band and 2.6 kW for each of the higher bands. Thus, the AA and AC cooling systems constituted a very wide-band, high-power, low-noise, cryogenic HiFi scheme, with feedthroughs and fast-moving electrodes in ultra-high vacuum.

The art of stacking by stochastic cooling and the solution adopted for the AA are described in the literature [25, 26]. Stacking is done in momentum space: The pickups are located in regions of

large dispersion, where particles are radially separated according to their momentum. Partial-aperture cooling systems acted over different aperture regions. The overall gain was profiled to decrease roughly exponentially from the low-density stack-tail (high gain) to the high-density core, by a factor comparable to the density ratio of 105. Loop couplers were used for the tail and Falin-type slotted TEM lines [27] for the core. In the original AA, bands of 250 MHz to 500 MHz and 1 GHz to 2 GHz were used for tail and core cooling, respectively.

When later pre-cooling was done in the AC, simplifications became possible in the AA. In particular, shutters on the injection kicker and on the cooling devices at the injection orbit were no longer needed. Transverse cooling was less demanding, as beams of already low emittance arrived from the AC. On the other hand, the higher intensity and density put greater demands on stack cooling. The performance was improved by further momentum pre-cooling on the AA injection orbit and by a powerful transverse stack-core cooling system using partly the difference signal from the momentum systems. All cooling systems were replaced by higher frequency ones. More details can be found in the parameter lists [22, 23].

3.5 Accumulator performance

During its initial years of operation the AA performance progressed steadily. Routine operation was attained in 1982. For AC and AA together, this was the case in 1988. Table 2 reflects the performance in 1984 [22] and in 1994 [23]. Most impressive is the increase of phase space density (8–9 orders of magnitude) that was consistently obtained during cooling and accumulation.

Table 2: Operational performance of AA (in 1984) and AA + AC (in 1994)

| Characteristic | Original AA (with horn) | AC + AA (with 20 mm lithium lens) |
|--|----------------------------|--------------------------------------|
| 26 GeV/c protons per pulse on target | 1.2×10^{13} | 1.4×10^{13} |
| Antiprotons per pulse injected $N_{\bar{p}}$ | 6.7×10^6 | 7.3×10^7 |
| Yield $N_{\bar{p}} / N_p$ | 5.6×10^{-7} | 5.2×10^{-6} |
| Antiprotons stacked per injection | 4.7×10^6 | 6.0×10^7 |
| Best daily production $N_{\bar{p}} / 24h$ | 1.7×10^{11} | 1.1×10^{12} |
| Largest stack attained $N_{\bar{p}-stacked}$ | 2.8×10^{11} | 1.3×10^{12} |
| Corresponding stacking factor | 6.0×10^4 | 2.2×10^4 |
| Increase of phase-space density | 5.4×10^8 | 4.3×10^9 |

4 The antiproton decelerator

By 1994 it had become evident that one could not afford for much longer the complex and costly operation of LEAR for low-energy antiproton physics (involving PS, AC, AA, again PS, and LEAR). The desire of the users' community to continue the highly interesting physics with low-energy antiprotons initiated a search for a substitute facility, which would satisfy at least part of the program, such as the production of antihydrogen.

Studies [28, 29] resulted in the following scheme: the target area would remain as it was; the AA would be removed; the AC would be modified to be ramped from the injection momentum of 3.5 GeV/c down to 100 MeV/c; only fast ejection of antiprotons in a single bunch of about 10^7 antiprotons every minute would be provided. Compared with LEAR, one had to accept a large decrease (factor 10) in antiproton flux and the lack of ultraslow extraction, but the number of machines involved was reduced from five to two and the operational burden greatly relieved.

In 1997, the AA was dismantled and the conversion of the AC into the AD started. Apart from the magnetic aspects, it is the adiabatic increase of beam emittance during deceleration that posed the greatest challenge. The beam has to be cooled, not only right after injection, but also on intermediate plateaus. The AC stochastic cooling system was therefore adapted for additional use at 2 GeV/c. Electron cooling had to supplement it at lower energies.

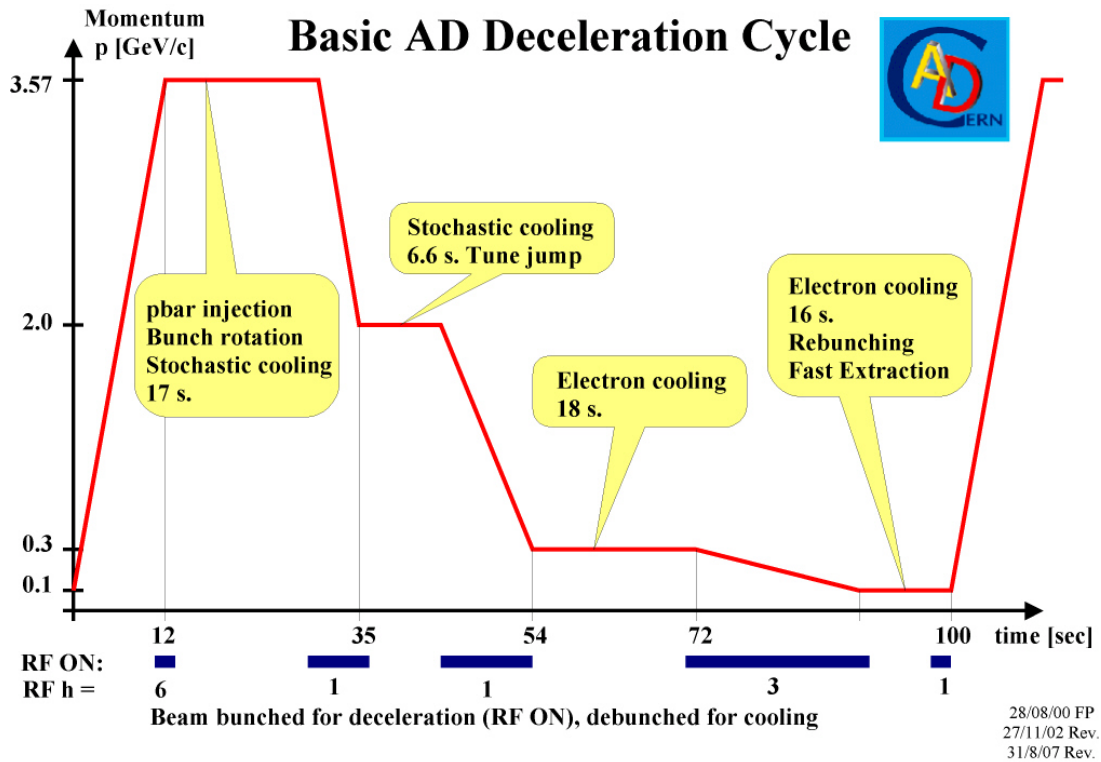


Fig. 8: A typical AD cycle

A typical cycle [30] is shown in Fig. 8. Upon injection, the antiprotons fill the acceptances. Bunch rotation reduces the momentum spread and lengthens the bunches, whereupon stochastic cooling in all three phase spaces reduces the transverse emittances and the momentum spread. This now permits deceleration to 2.0 GeV/c, where further stochastic cooling is applied, allowing the next deceleration to 300 MeV/c. Now electron cooling is called upon before the last deceleration to 100 MeV/c and final electron cooling reduces the beam to very small emittances. The beam is then rebunched and rotated in longitudinal phase space by RF, whilst cooling continues, to provide a bunch

of only 90 ns to 200 ns length as required by the trap experiments, still with a $\Delta p/p$ of a few 10^{-4} . In this way, some 10^7 antiprotons are provided for the experiments every 100 s. In November 1999, the first 100 MeV/c antiprotons were sent to the ASACUSA experiment. In 2000 operation started in earnest, with beams given to three experiments. Since 2001 the AD has reliably worked for 6 or 7 months every year. This led to continuous improvement of the trapping efficiency of antiprotons by the experiments and, since 2010, to trapping of antihydrogen atoms for spectroscopy. This will make a high-precision comparison with normal hydrogen spectra (CPT test) possible.

Deceleration of antiprotons in the AD goes a long way towards the needs of the experimenters, but the 5.3 MeV kinetic energy of the extracted beam is still far above what the trap experiments require. The further deceleration in a degrader foil, still in use for two of the AD experiments, is accompanied by a big loss of density. A decelerating RF quadrupole [31] was constructed and put into service in 2001 for one of the experiments (ASACUSA). It slows down the antiprotons to an energy which can be chosen between 10 keV and 120 keV. This leads to a sizable beam density improvement at the output but still exhibits the adiabatic increase in density during deceleration from 5.3 MeV to the low-energy range.

In order to substantially increase the density, an additional “Extra Low Energy Antiproton ring” (ELENA) [32] post-decelerating the AD beam from 5.3 MeV to 100 keV was approved in June 2011. ELENA, having a circumference of about 30 m, will be constructed in the AD hall. It will use electron cooling to counteract the adiabatic density increase and it is planned to be ready in 2015.

5 Conclusions

Originally the driving force for the construction and operation of the antiproton rings was the strong desire to finally prove the existence of the intermediate bosons. Subsequently, the project opened the rich field of low-energy antiproton physics, which prospers still today, 20 years after the shut-down of the Collider experiments. There is no doubt that the success of the antiproton programme, as another demonstration of CERN's accelerator competence, has greatly furthered the adventure of the Large Hadron Collider (LHC).

The AA, AC, LEAR and AD were all constructed and operated under the responsibility of the PS Division and are, at present, operated by the Beams Department (BE). Yet from the beginning, throughout the definition of the project and the construction and the operation of the rings, there was an intense and most fruitful collaboration between the accelerator experts and the experimenters across all of the divisions involved. This breaking of the barriers was a source of motivation, which, no less than the scientific and technical effort and ingenuity, was essential for reaching success.

References

- [1] K. Johnsen, Opening remarks, in: P. Bryant, S. Newman (Eds.), Proc. CERN Accelerator School, 1983, Antiprotons for Colliding Beam Facilities, CERN 84-15, 1984, p. 1.
- [2] G.I. Budker, Status report of the work on storage rings at Novosibirsk, Proc. Symp. International sur les Anneaux de Collision, Saclay, 1966, Eds. H. Zyngier and E. Cremieu-Alcan (Presse Universitaire de France, Paris, 1966), p.II-1-1.
- [3] S. van der Meer, Stochastic damping of betatron oscillations in the ISR, CERN Int. Report ISR-PO/72-31 (1972).
- [4] G.I. Budker *et al.*, *IEEE Trans. Nucl. Sci.* **22** (1975) 2093.
- [5] P. Bramham *et al.*, *Nucl. Instrum. Methods* **125** (1975) 201.

- [6] C. Rubbia, P. McIntyre and D. Cline, Producing massive intermediate vector bosons with existing accelerators, Proc. International Neutrino Conf., Aachen, 1976 (Vieweg Verlag, Braunschweig, 1977), p. 683.
- [7] G. Carron *et al.*, *Phys. Lett.* **77B** (1978) 353.
- [8] P. Strolin, L. Thorndahl, D. Möhl, Stochastic cooling of antiprotons for ISR physics, CERN Int. Report EP 76-05 (1976).
- [9] M. Bregman *et al.*, *Phys. Lett.* **78B** (1978) 174.
- [10] AA design study team, Design of a proton–antiproton colliding beam facility, CERN Int. Report PS/AA 78-3 (1978).
- [11] L. Evans, E. Jones and H. Koziol, The CERN $p\bar{p}$ Collider, in *Proton–Antiproton Collider Physics*, Eds G. Altarelli and L. di Lella (World Scientific, Singapore, 1989).
- [12] E.J.N. Wilson (Ed.), Design study of an Antiproton Collector for the Antiproton Accumulator, CERN 83-10 (1983).
- [13] H. Koziol and D. Möhl, *Phys. Rep.* **403–404** (2004) 271.
- [14] J. Allaby, Antiproton production, in: P. Bryant S. Newman (Eds.), Proc. CERN Accelerator School, 1983, Antiprotons for Colliding Beam Facilities, CERN 84-15, 1984, p.63.
- [15] C. Hojvat and A. van Ginneken, *Nucl. Instrum. Methods* **206** (1983) 67.
- [16] M.D. Church and J.P. Marriner, *Ann. Rev. Nucl. Part. Sci.* **43** (1995) 253.
- [17] S. van der Meer, Improved collection of secondaries from a long, narrow target by a horn doublet, CERN Int. Report PS/AA 80-12 (1980).
- [18] D. Boimond, *et al.*, Consolidation of the 400 kA magnetic horn for AAC antiproton production, CERN Int. Report PS 94-02-AR (1994).
- [19] R. Bellone, *et al.*, Beam tests of a 36 mm lithium lens, Proc. Second European Particle Accelerator Conf. (EPAC '90), Nice, France, 1990, p.1303
- [20] R. Bellone, *et al.*, Performance and operational experience with CERN-lithium lenses, Proc. First European Particle Accelerator Conf. (EPAC '88), Rome, 1988, p. 1401.
- [21] R. Kowalewicz, *et al.*, Beam tests with the CERN plasma lens, Proc. Third European Particle Accelerator Conference, EPAC '92, Berlin, 1992, p. 1539.
- [22] H. Koziol, Antiproton Accumulator (AA) Parameter List, 9th Edition, CERN Int. Note PS/AA/Note 80-2, 1980; 10th Edition, CERN Int. Note PS/AA/Note 84-2 (1984).
- [23] S. Maury, H. Koziol, Parameter list for the Antiproton Accumulator Complex (AAC), CERN Int. Report /PS 95-15 (AR/BD) (1995).
- [24] G. Carron and L. Thorndahl, Stochastic cooling of momentum spread with filter methods, CERN Int. Report /ISR-RF/ 78-12 (1978).
- [25] S. van der Meer, Stochastic stacking in the Antiproton Accumulator, CERN Int. Report PS/AA 78-22 (1978).
- [26] F. Caspers and D. Möhl, *Nucl. Instrum. Methods* **A532** (2004) 321.
- [27] L. Faltin, *Nucl. Instrum. Methods* **148** (1978) 449.
- [28] S. Maury and D. Möhl, Simplified schemes for Antihydrogen production in traps, CERN-PS/AR Note 95-17 (1995).
- [29] S. Maury *et al.*, Design study of the antiproton decelerator; AD, CERN PS 96-43(AR) (1996).
- [30] P. Belochitskii, *AIP Conf. Proc.* **821** (2006) 48.
- [31] A.M. Lombardi, W. Pirkel and Y. Bylinsky, First operating experience with the CERN decelerating RFQ for antiprotons, Proc. 19th IEEE Particle Accelerator Conf., Chicago, IL, June 2001, p. 585
- [32] T. Eriksson *et al.*, ELENA: An Updated Cost and Feasibility Study; CERN-BE-2010-029.

The Low-Energy Antiproton and Ion Rings LEAR and LEIR

1 Introduction

Stimulated by the ideas for the SPS $p\bar{p}$ Collider, Kilian *et al.* [1] realized in 1976 that cooling and deceleration of antiprotons would provide beams of unprecedented intensity and purity for low-energy physics. This led to the proposal to add a small facility [2] to the antiproton project for experiments with cooled \bar{p} beams in the energy range of 5 MeV to 1200 MeV. The proposal received enthusiastic support and, in 1980, the Low Energy Antiproton Ring (LEAR) project [3] was launched.

LEAR was built in the old PS South Hall, which also served as its experimental area, and antiprotons were first delivered to users in June 1983. After the end of the SPS Collider programme in 1991, LEAR remained the only user of the Antiproton Collector (AC) and the Antiproton Accumulator (AA). Its unique but complex and costly operation continued until November 1996. Figure 1 shows the PS complex in the 1990s, before the final transformation of the \bar{p} machines. In 1997, in fact, the CERN AC was dismantled and the AA was converted into the Antiproton Decelerator (AD) [4], a simplified all-in-one ring, for low energy \bar{p} operation.

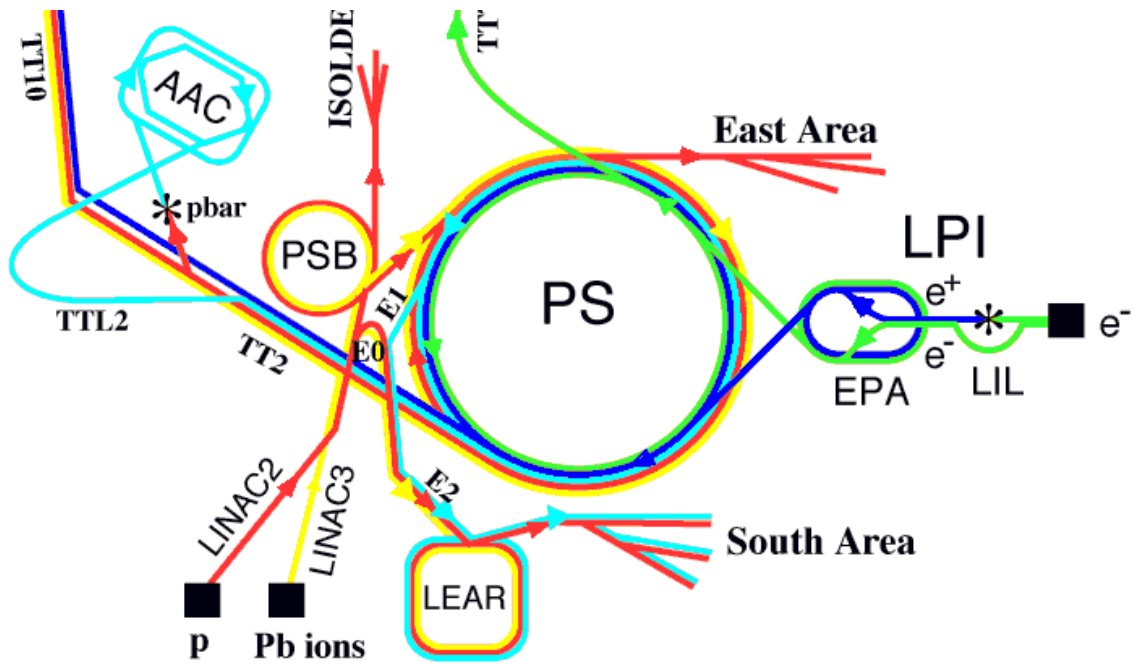


Fig. 1: General layout of the PS complex in the 1990s

In 1993 it was proposed to use “a ring-like LEAR” to accumulate heavy ions for injection to the Large Hadron Collider (LHC) [5]. The idea is to gain a very large factor in beam intensity and density by cooling and stacking the ions from the Linac 3 prior to injection in the PS. LEAR was used extensively (especially during 1997 when its antiproton program had already stopped) to test the required techniques [6]. In 2006 the ring was converted “*in situ*” and began a new career as a Low Energy Ion accumulation Ring (LEIR) for the LHC [7–9].

In the following we give a brief description of the accelerator aspects of the low energy antiproton and ion ring. Readers interested in more detail are referred to Refs. [2, 3, 10, 11] for LEAR and Refs. [7–9, 12–16] for LEIR.

2 LEAR

2.1 The magnet lattice

LEAR (Figs. 2 and 3) is almost square in shape with a circumference of 78 m (1/8 of the PS). Its four-period lattice with compact 90° bending magnets and eight quadrupole doublets provides four long straight sections, each of 8 m free length. These served for the installation of large equipment, in particular the electron cooler and the internal gas jet target experiments. Eight short straight sections, 1 m long each, accommodate less bulky equipments. The C-type magnets are open to the outside of the ring. This choice simplified injection, ejection, and the design of “exit lines” for neutral states formed in flight in the straight sections (\bar{H}_0 , antineutrons, $\bar{p}p$ -bound states). The exit lines greatly eased the detection of antihydrogen atoms formed by \bar{p} interaction with an internal gas target. It was therefore not completely unexpected, when antihydrogen atoms were experimentally observed at LEAR (for the first time in human history) in 1996 [17], an event that was widely covered by the media.

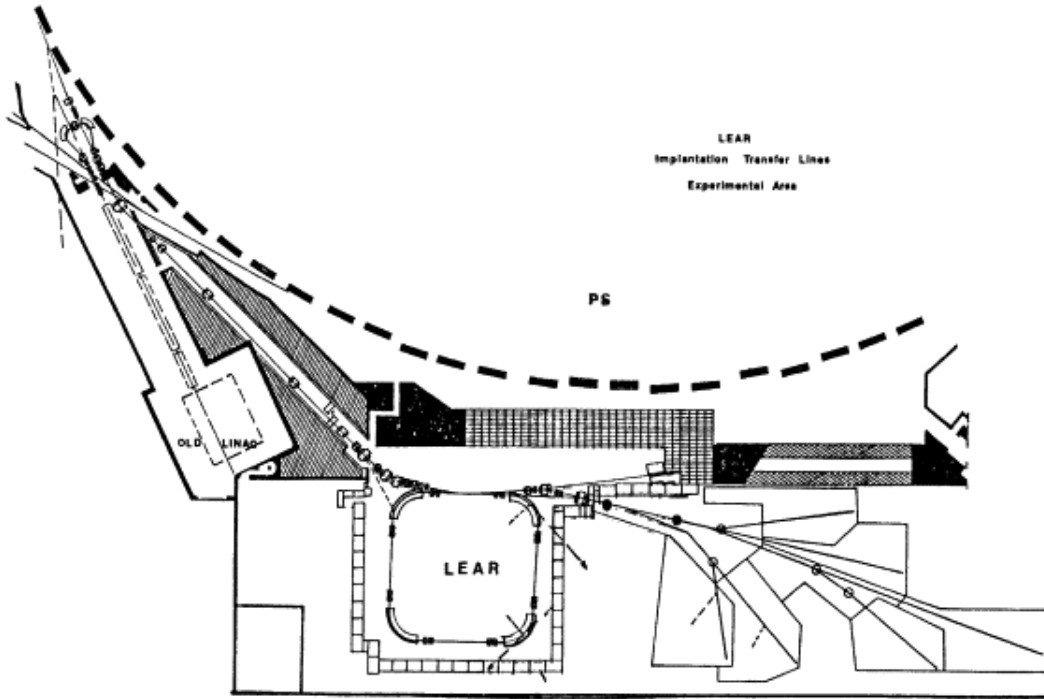


Fig. 2: Layout of LEAR in the PS South Hall, with injection lines (test-proton and H^- from the Linac, antiprotons from the PS), and the lines transporting ejected antiprotons towards the experiments (status 1984).

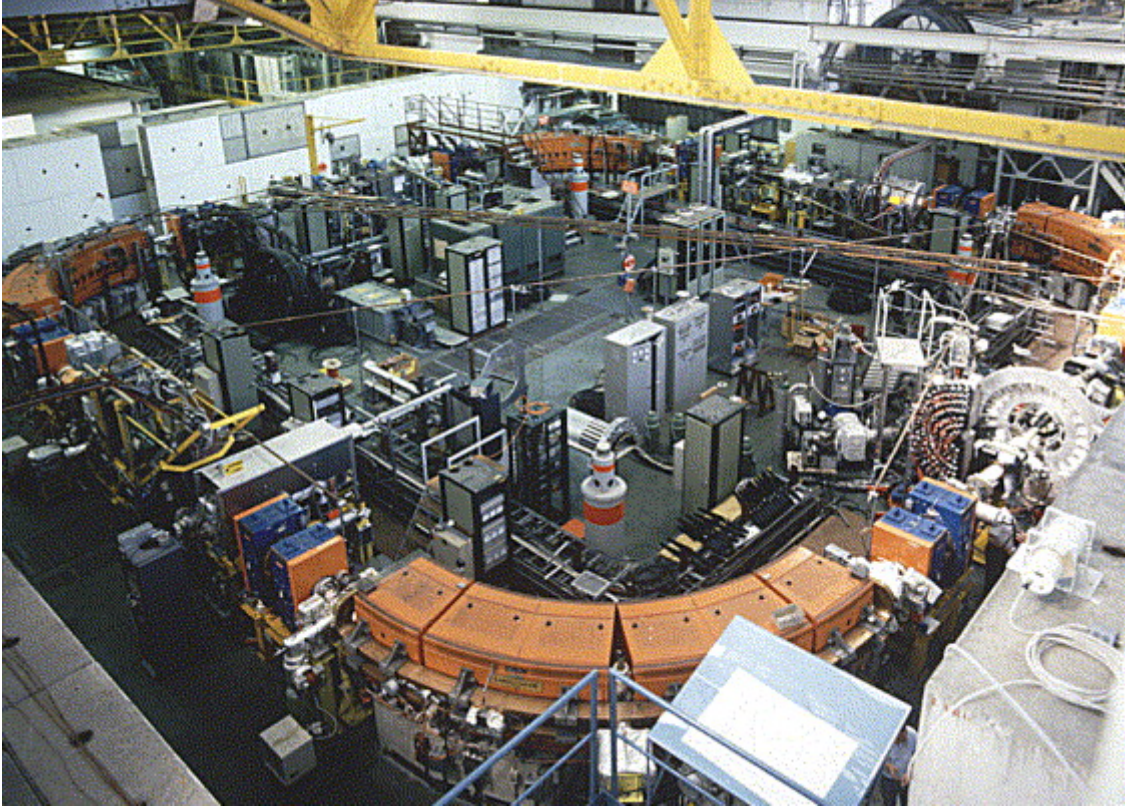


Fig. 3: LEAR in the PS South Hall (1990). Clockwise from the bending magnet in the foreground, the four long straight sections (SS) house: electron cooling (SS3); RF cavities (SS4); injection and ejection (SS1); the internal gas jet target experiment JETSET (SS2). The detector of JETSET is partially dismantled. A web of coaxial transmission lines for stochastic cooling spans across the ring.

A particularity of the LEAR optics was the very strong focusing: a phase advance of $\sim 250^\circ/\text{period}$ yielded an “imaginary transition energy” (*decrease of orbit length C with momentum*, i.e. negative momentum compaction ($(dC/C)/(dp/p) \equiv \alpha_p = \gamma_{tr}^{-2} < 0$). This avoids transition and also leads to a large dispersion of the revolution frequencies $\eta \equiv (df/f)/(dp/p)$, beneficial for cooling to small momentum spreads and for control of instabilities. Other important features of LEAR were the ultra-high vacuum, 10^{-12} Torr, for sufficient beam lifetime at low energy and, as described below, beam cooling and ultra-slow extraction.

2.2 The operating scheme

A single bunch, of usually a few 10^9 antiprotons, was skimmed off the AA stack at intervals ranging from 15 minutes to several hours. The average consumption, $10^6 \bar{p}/s$, was only 10% of the maximum accumulation rate of the AA. The bunch was decelerated in the PS to 609 MeV/c and transferred to LEAR, where it could either be decelerated to as low as 100 MeV/c (5.3 MeV kinetic energy), or accelerated, up to nominally 2000 MeV/c (1270 MeV).

In the “beam stretcher mode”, used for most of the experiments, ultra-slow extraction provided a continuous spill until the next fill. In the “internal target” mode for the JETSET experiment, a beam with an initial intensity of as much as $5 \times 10^{10} \bar{p}$ was kept circulating for many hours, even days, until most particles had been consumed by interaction with the gas jet target. For trap experiments, one or several bunches were extracted by a fast kicker.

2.3 Cooling

Stochastic cooling of all three emittances was optimized for several strategic momenta: 609 MeV/c (injection), 300 MeV/c, 200 MeV/c and 100 MeV/c on the low-energy cycle and 1000 MeV/c, 1500 MeV/c and 1940 MeV/c on a high-energy cycle. Cooling compensated for the adiabatic emittance growth during deceleration and counteracted various heating mechanisms, such as multiple Coulomb scattering, notably on the internal targets of the JETSET experiment. Final cooling was applied at the momentum at which the beam was delivered to the users, to provide a highly monochromatic and small-sized beam.

A complex cooling system with a great number of different pickups and kickers and containing a plethora of switchable delays was necessary to permit cooling at all momenta. For sufficient signal level, the pickup arrays had to be long. As much as possible they were installed inside the vacuum chamber in the bending magnets where space was “cheap”. An ever-growing web of coaxial lines was spun across the ring for the transmission of the signals from pickups to kickers. Diagonal paths were necessary for cooling at high energy to catch up with the particle velocity $\beta = v/c \approx 1$. For low energy, shorter paths were possible and favourable to avoid de-synchronization between off-momentum particles and their correction signal (“unwanted mixing”).

From 1987, electron cooling complemented stochastic cooling. The electron cooler, which had served until 1979 in the Initial Cooling Experiment (ICE), was resuscitated and upgraded for service in LEAR at momenta between 300 and 100 MeV/c. This device has even survived LEAR and now operates in the AD.

The combination of both cooling methods pioneered in LEAR lead to very high-quality beams at low energy with emittances as low as space charge and instabilities permitted, typically $10^9 \bar{p}$ with $\varepsilon \sim 1 \pi \text{ mm mrad}$ and $\Delta p/p \sim 10^{-4}$. Elaborate stabilization systems were needed to hold beam instabilities in check.

2.4 Ultra-slow extraction

In the stretcher mode, a spill as constant as possible of some $10^6 \bar{p}/s$ was required by the users. The filling sequence was determined by the smallest intensity that the PS was able to handle. The limit was pushed down to $10^9 \bar{p}$, some four orders of magnitude below its usual value for protons. Even so, the spill length had to be at least 15 minutes, a formidable challenge, as so far extraction times of only a few seconds had been achieved. It meant beam stretching (“extraction time/revolution time”) of nine orders of magnitude with, on average, less than one particle extracted per turn. A novel ultra-slow extraction technique was devised for this purpose. It is based on yet another idea by van der Meer [18], which was brought to maturity by Hardt *et al.* [19].

Conventional slow extraction uses a programmed tune change, driving the beam towards a resonance, which eats into the tune distribution of the beam. The time structure of the spill is very sensitive to all sorts of tune ripple and exhibits spikes and holes (detrimental to the experiments) when the sweep is slow.

Ultra-slow (“stochastic”) extraction uses radiofrequency (RF) noise to diffuse the particles within an appropriate range of $\Delta p/p$, thereby producing a very-low-density tail on the momentum distribution. The chromaticity, $dQ/(dp/p)$, adjusted with sextupole lenses, leads to a corresponding tail in the Q -distribution and the extraction resonance is placed at a Q -value inside that tail. This largely reduces the influence of Q -ripple, as the density near the resonance is low and particles perform a random walk around it. The spill rate is controlled by the level of the noise transporting particles from the stack into the tail.

This concept worked admirably well and permitted good 15 minute spills in the first runs in 1983. Very soon, 1 hour spills became common. At the end of the LEAR era, the number of transfers per day was minimized by taking from the AA batches of the highest intensity compatible with safe operation for the experiments. Figure 4 illustrates a 10 hour spill; the record spill length was 14 hours.

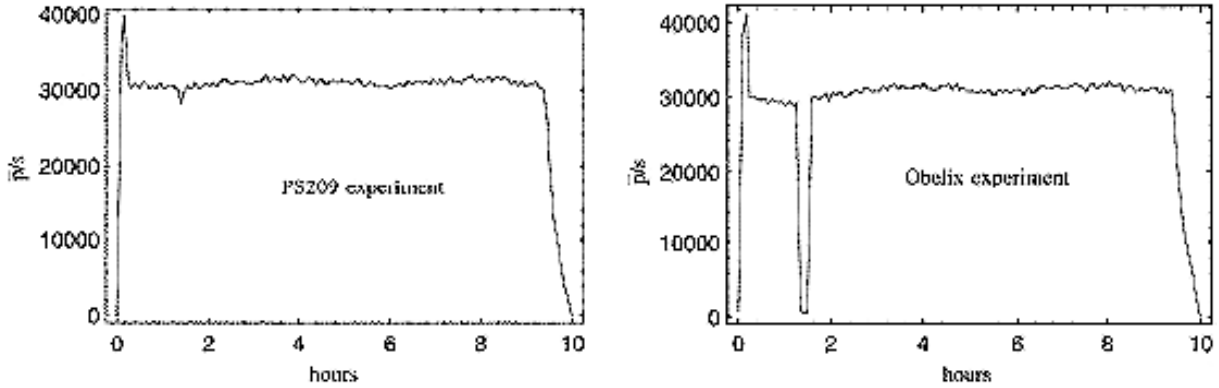


Fig. 4: A typical spill in the ultra-low extraction, lasting 10 hours. The beam is shared by two experiments (a "splitter magnet" divides the extracted beam). Each point on the curve represents the rate recorded by the experiments, averaged over 10 s. The brief interruption in the counting rate of OBELIX was for recalibration.

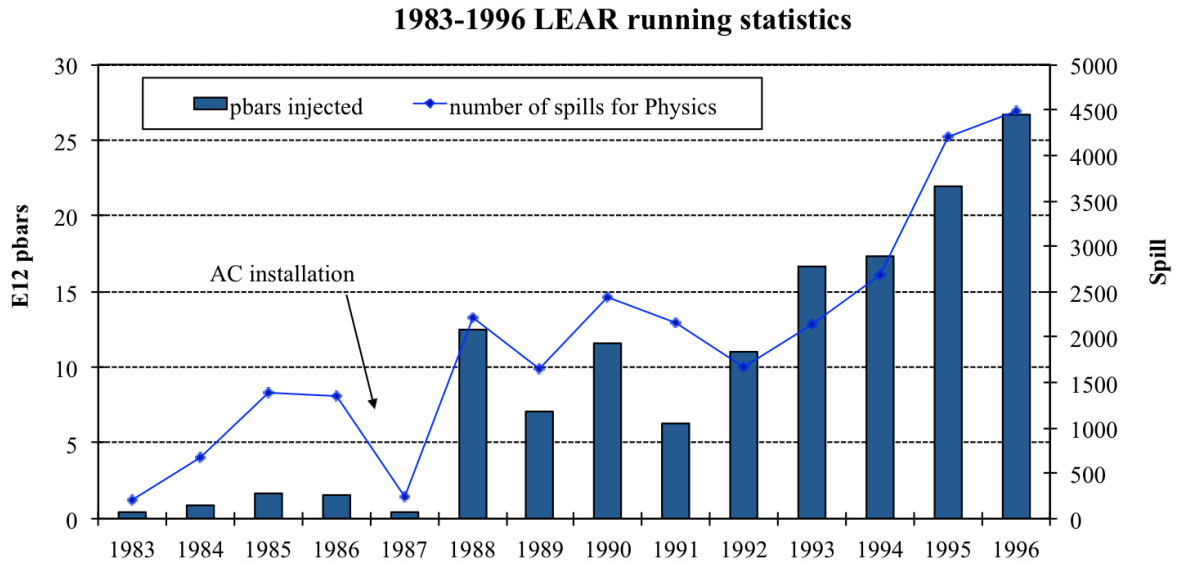


Fig. 5: LEAR operation statistics from 1993 to 1996. Number of antiprotons injected (bars) and number of spill delivered (small squares).

2.5 Performance

During the 14 years of operation, the number of antiprotons consumed by LEAR increased from a few 10^{11} to 2.6×10^{13} per year (Fig. 5). The step in 1987/88 is due to the advent of the AC. Another step occurred in 1991/92 when LEAR became the only client of the AC/AA. The total number of antiprotons supplied was around 1.5×10^{14} (0.24 ng).

The number of scheduled hours increased from 283 in 1983 to an impressive 5450 in the final year, 1996. The number of spills delivered to the users was usually 90%, and always more than 85%, of those scheduled.

3 LEIR

3.1 The feasibility tests

After the proposal [5] to have a ring to accumulate lead in view of the LHC ion program, many feasibility tests were conducted through the years 1994 to 1996 and finally during the whole year in 1997 [6]. The main results of these tests were very important for the final design of the machine:

- The possibility to combine a longitudinal and horizontal multiturn injection was tested successfully.
- It was found that the lead 53^+ ions were subject to dielectronic recombination with the electrons of the electron cooler, leading to large losses and hence a poor ion accumulation rate. In contrast to this, lead 54^+ ions were found to be suitable for accumulation as they showed considerably lower losses. The same phenomenon was also observed for gold ions (with the same remaining number of electrons) at TSR [20] and precisely analysed for lead ions at CRYRING [21].
- On the other hand, the radiative recombination was found, as expected, due to the very good vacuum (quantity and quality) in LEAR, the charge exchange recombination was found to be very low. Nevertheless the lost lead ions bombarding the vacuum chamber walls released a lot of molecules into the vacuum, mainly carbon oxide (a few 10^4 atoms/lost ion) [6, 22, 23]. This phenomenon was indeed detrimental to the accumulation rate and limited the maximum number of accumulated ions.
- A lot of cooling and stacking measurements [6] were executed too. They established the feasibility to accumulate ions in LEAR, provided that an adaptation of the lattice is made to inject, cool and stack efficiently.

3.2 The machine

Operation of LEIR sets several requirements on the optics:

- Injection: a relatively large normalized dispersion $D/\beta^{1/2}$ is needed for the elaborate multiturn injection [24] with stacking in momentum and both horizontal and vertical phase spaces. The value obtained ($D/\beta^{1/2} \approx 5$) is a bit smaller than desired.
- Electron cooling: betatron functions of about 5 m were found to be optimal for fast electron cooling [6]. Although a finite dispersion of a few metres was found to be beneficial for a fast cooling, it has been decided to have zero dispersion for easy overlap of ions (with large momentum spread at injection) with electrons. In addition, the extraction installed in the opposite straight section will profit from the zero dispersion.
- Working point: operation far from ($Q_H - Q_V = -1$) resonance and clear from other dangerous resonances was required to obtain good multiturn injection efficiency and avoid emittance blow-up.
- Aperture: sufficient momentum and transverse acceptances had to be provided.
- Ion beam lifetime: it should be as high as 15 s to be able to accumulate more than 10^9 lead ions in about a second.
- Multibeam operation: two kinds of beams have to be delivered. The EARLY beam is needed for the starting phase of collision in LHC. It is composed of one bunch per LEIR cycle containing 2.2×10^8 ions. The NOMINAL beam is composed of two bunches containing 4.5×10^8 ions each and is needed when LHC will be in full operation.

3.2 General layout and the “bare” machine

LEIR inherits its “square” shape (see Fig. 6) from the former LEAR. Quadrupole doublets are installed in the injection Straight Section 10 (SS10) and opposite in SS30. Triplets are used in SS20 on both sides of the electron cooler and in the opposite SS40 suited for extraction. The basic focusing is defined by five quadrupole families, which surprisingly are sufficient to yield a lattice satisfying all of the requirements given above.

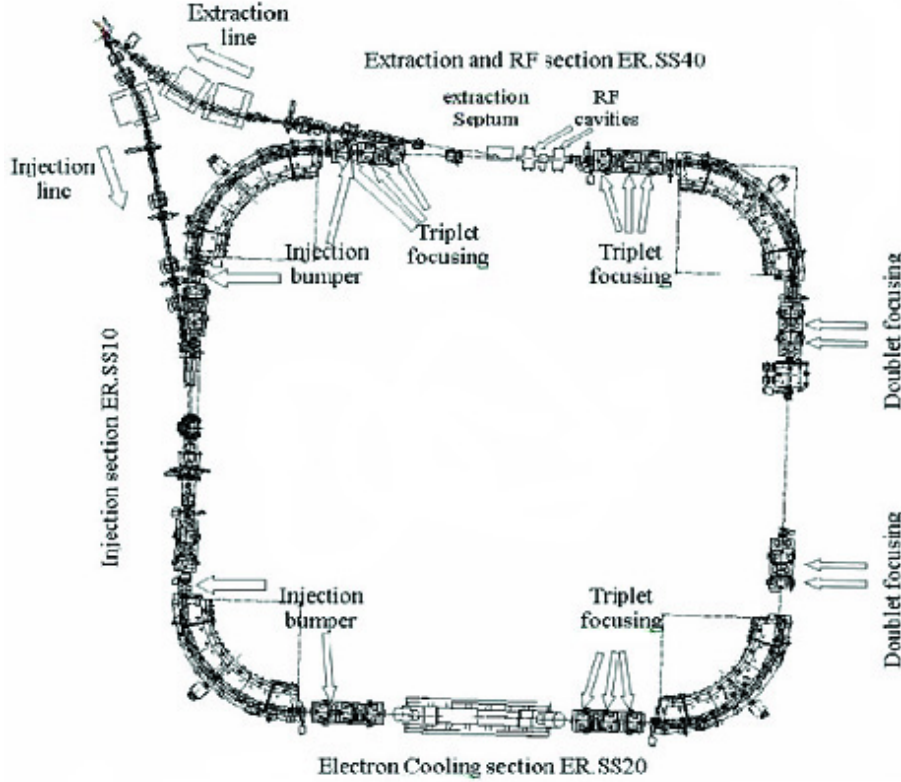


Fig. 6: Layout of the LEIR ring

3.3 Compensation of the electron cooler

The cooler introduces a strong source of coupling due to the longitudinal magnetic field of the main solenoid. The electron cooler magnet system has no azimuthal symmetry in the toroids. The coupling introduced is compensated mainly by two solenoids placed symmetrically on either side of the cooler. In order to compensate for the small skew quadrupole components in the toroids and the residual coupling of the machine, skew quadrupoles are used. They are located symmetrically within the triplets. In order to compensate for the changes of the working point and the betatron functions caused by the cooler and other coupling elements, corrections to the five quadrupole families and to the setting of the triplet quadrupoles in SS20 via trim power supplies are programmed. The corrections depend quadratically on the ratio between the solenoidal field and the beam rigidity, and are reduced during acceleration.

3.4 Eddy current compensation

The LEIR bending magnets are C-shaped and the vacuum chamber is connected to ground at various locations. As a consequence, a net eddy current flows along the chamber during the ramp resulting in a gradient experienced by the beam. It produces strong tune shifts, especially in the horizontal plane, where the working point moves below the half-integer resonance. This perturbation (together with the

distortion of betatron functions around the ring) has to be compensated by adding appropriate corrections to the five main quadrupole families.

3.4.1 *Beam lifetime*

The electron beam [25] of the cooler can have a non-uniform density distribution (programmed by a control electrode): less density in the centre, where the stack sits, to limit the recombination of ions with cooling electrons, and thereby the ion losses; a higher density elsewhere to allow a fast cooling for the particles having large amplitudes of oscillation. Nevertheless to limit the outgassing of the vacuum chamber walls, the major part of the remaining losses are concentrated onto a collimator system [26]. Two parameters were essential: the impact angle has to be close to 90° ; the collimators are made of stainless steel coated with $30\text{ }\mu\text{m}$ of gold. In addition, the vacuum system has been carefully improved by coating the vacuum chamber wherever possible with low temperature NEG's. As for LEAR the LEIR machine is baked to $300\text{ }^\circ\text{C}$.

3.4.2 *Particularities*

Amongst the particularities, let us note the following:

- Part of the injection line (from Linac 3 to LEIR at 4.2 MeV/n) and the extraction line (from LEIR to the PS at 72 MeV/n) is common. To avoid bipolar power supplies for the quadrupoles, a special arrangement of the lattice was made, leading to quadrupoles which are defocusing for extraction when focusing for injection and vice versa.
- The multiturn injection is made through an inclined septum (30°) with horizontal and vertical mis-steering, to avoid as much as possible ions hitting the septum. The horizontal oscillation is maintained constant by increasing the incoming beam momentum and decreasing accordingly the local injection bump. This provides a 70 turns injection ($200\text{ }\mu\text{s}$ long) with a 60–70% efficiency.
- New at CERN, but used for a long time in other laboratories [27], the multi-injection with stacking–cooling sequence has been imported.
- The lattice super-symmetry is only two and, in addition, it is heavily distorted by the electron cooling insertion. As a consequence there are a large number of parameters to be controlled by the five quadrupole families and the many trim power supplies. In contrast to the LEAR machine, the LEIR transition energy is “real” ($\sim 2.5\text{ GeV}$).
- Owing to the low energy of the particles, the swing in frequency is large and, in addition, multiharmonic operation can be used (RF range $0.5\text{--}5\text{ MHz}$). This lead to the use of low-quality factor RF cavities, made in collaboration with KEK, and loaded with Finemet® magnetic alloy cores. The low-level beam control of the RF system is, for the first time at CERN, completely digital.
- The commissioning of LEIR had to be done just before the commissioning of the LHC. Then, it was a good opportunity to investigate in LEIR many of the processes which will be used at LHC. Amongst them, the FESA technology, the LSA machine parameters editor and trim, the WIC magnet protection system and the LASER fault diagnostic system were tested extensively.

3.5 The LEIR performance

3.5.1 From the commissioning to the first operation run

After a long period of setting up the different systems, the machine was first tested with O^{4+} in 2005. The lattice functions were analysed by orbit response to small kicks and proved to be close to the design values [12, 13].

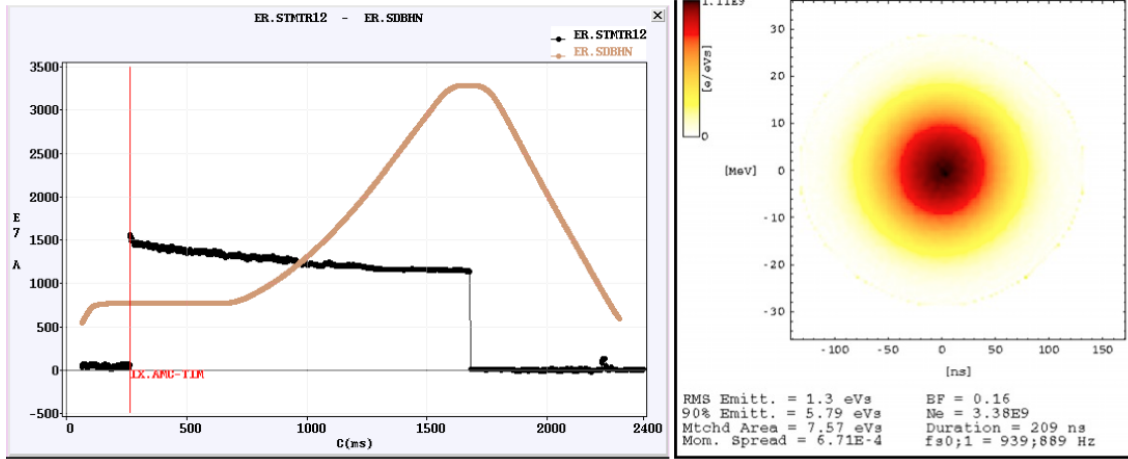


Fig. 7: LEIR performance for the “EARLY” beam used routinely for setting up of the PS and SPS. The evolution of the beam current (left) and a tomographic reconstruction of the longitudinal phase space (right) are shown.

Ring commissioning resumed in the middle of February 2006 with Pb^{54+} ions. At the very beginning, progress was slowed down by difficulties in tuning the injection efficiency with lead ions, again due to problems with injection matching. After improving the injection line setting [12] and setting up of the transverse damper, clear signs of cooling could be observed on 3 March without particular difficulties. LEIR commissioning has been completed, almost as scheduled, in May 2006 with the proof that the EARLY LHC ion beam could be produced (Fig. 7) and transported to a region just upstream from the PS injection.

The first regular LEIR run has taken place in autumn 2006 in order to provide the beam for setting up the PS with the “early LHC ion beam”. The second LEIR run started at the beginning of August 2007. Again, the start-up was carried out without particular difficulties and LEIR soon delivered routinely the beam needed for SPS setting up.

3.5.2 Actual LEIR performance

Table 1 compares LEIR performance as observed during the last 2009 run with design values for the EARLY beam needed for the first LHC ion runs and the NOMINAL beam. One observes that the design performance has been reached for the EARLY beam with transverse emittances significantly below specifications. Figure 7 (left) shows some details.

After injection, a bit more than the design intensity is circulating. With some losses mainly during the cooling plateau, the design intensity is ejected. The tomographic reconstruction of longitudinal phase space shows that the design longitudinal emittance is reached. The number quoted in Fig. 7 (right) is the root mean square for all 208 nucleons.

Figures 8 and 9 show some measurements for high-intensity beams. With high Linac 3 currents, intensities, exceeding the design value at ejection, have been obtained. However, the evolution of the beam current shows a loss at the beginning of the ramp.

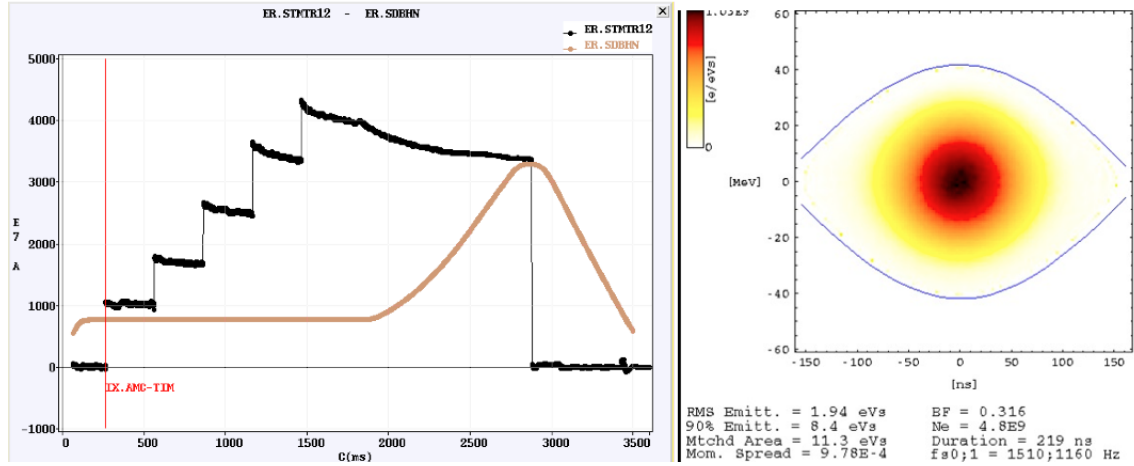


Fig. 8: LEIR performance with a high-intensity beam. The evolution of the beam current (left) and a tomographic reconstruction of the longitudinal phase space (right) are shown.

Table 1: Comparison of LEIR design and obtained performance for the nominal beam and the beam needed for the early LHC ion runs

| Parameter | NOMINAL | | EARLY | |
|--|---------|-------------------|--------|------------|
| | design | obtained | design | obtained |
| Linac 3 current [μA] | 25 | 25 | 25 | 25 |
| Cycle time [s] | 3.6 | 3.6/4.8 | 2.4 | 2.4 |
| Injection efficiency [%] | 50 | ~ 50 | 50 | ~ 50 |
| Accumulated intensity [10^8 Pb^{54+}] | | $\sim 10/\sim 15$ | | ~ 2.5 |
| Intensity for PS [10^8 Pb^{54+}] | 9 | $\sim 7/\sim 9$ | 2.25 | > 2.25 |
| Horizontal normalized emittance [μm] | 0.7 | 0.6/0.9 | 0.7 | 0.5 |
| Vertical normalized emittance [μm] | 0.7 | 0.3/0.5 | 0.7 | 0.24 |
| Long. emittance $4\pi \sigma_E \sigma_t$ per bunch [eVs/n] | 0.05 | 0.04 | 0.025 | 0.02 |

This loss is more pronounced for higher beam currents and, thus, the design current has not yet been obtained at ejection. However, investigations on these losses and of the NOMINAL LEIR beam are carried out only with low priority and in parallel to operation. The emittances in all three phase spaces are well within specifications. The EARLY beam has been accelerated up to the entrance of LHC while the NOMINAL beam has been commissioned in the PS and tested in the SPS.

Figure 10 shows that sufficient beam lifetimes (~ 14 s) for accumulating the nominal intensity have been obtained. During the 2006 run, intensities by more than a factor of two larger than the design nominal intensity have been accumulated on very long plateaus. Obviously these would never be possible without good performance of all systems, particularly the instrumentation [15, 16].

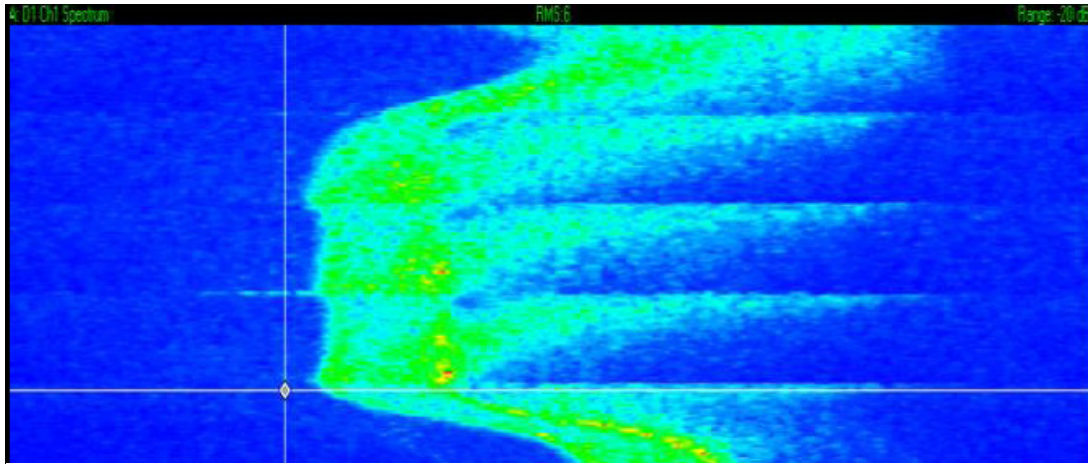


Fig. 9: Spectrogram of the momentum cooling during stacking on the injection front porch. The vertical and horizontal axis denote time (1.6 s total from top to bottom) and momentum spread (1% full scale). Injection is every 300 ms.

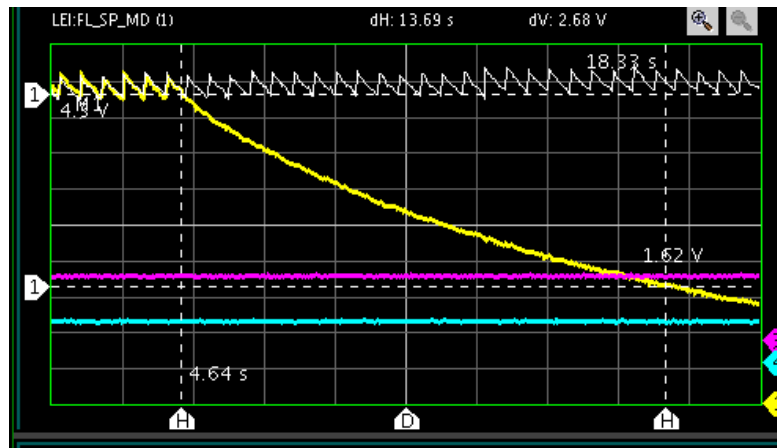


Fig. 10: Beam intensity (yellow trace) versus time (2 s/div) after accumulation on a very long plateau. The peak intensity is about 16×10^8 Pb^{54+} ions and the beam lifetime is about 14 s.

4 Conclusions

The low-energy antiproton programme had been conceived as an “adjunct” to the SPS Collider, at little extra cost and consuming only a small fraction of the antiprotons production, but the results obtained with LEAR soon made it an important and very visible part of CERN's activities. The interest was such that LEAR continued for 5 years beyond the end of the Collider. The AD then took over, and holds promise to deliver important physics contributions for several more years to come.

From the outset, the low-energy antiproton programme presented a major challenge to the accelerator community. LEAR was an unconventional enterprise, conceptually and technically. The success of the AA and LEAR has made the novel cooling, extraction and internal target approaches popular. It set the example for a dozen ion cooling rings (“king LEAR’s daughters”) built in Europe and the USA [27].

After the end of its programme, LEAR was rejuvenated as LEIR, an ion accumulator and beam shaper to prepare the bunches for LHC. It is now ready to provide the first lead ion beam to LHC at the end of the year 2010. It will be used also to provide ions for fixed target physics at SPS, and possibly for radiobiological experiment at the exit of LEIR. It is the promise of a long life with ions of different kind for interesting new discoveries.

Long live LEIR!

References

- [1] K. Kilian, U. Gastaldi and D. Möhl, Deceleration of anti-protons for physics experiments at low-energy: a low-Energy anti-proton factory, Proc. Tenth Int. Conf. on High-Energy Accelerators, Serpukov, Soviet Union, 1977, Eds. Yu.M. Ado, A.G. Afonin, V.I. Gridasov, A.F. Dunaitsev, E.A. Mjæe and A.A. Naumov (Protvino Institute of High Energy Physics, Serpukhov, 1977), p. 179
- [2] P. Lefevre, D. Möhl and G. Plass, The CERN Low Energy Antiproton Ring (LEAR) project, Proc. Eleventh Int. Conf. on High-Energy Accelerators, Geneva, Switzerland, 1980, Ed. W.S. Newman (Birkhäuser, Basel, 1980), p. 819.
- [3] G. Plass (Ed.), Design study of a facility for experiments with low energy antiprotons (LEAR), CERN-PS-DL-80-7 (1980).
- [4] S. Maury (Ed.), Design Study of the Antiproton Decelerator: AD, CERN-PS-96-043-AR (1996).
- [5] P. Lefevre and D. Möhl, Lead ion accumulation scheme for the LHC, Proc. Workshop on Beam Cooling and Related Topics, Montreux, Switzerland, 1993, Ed. J. Bosser (CERN, Geneva, 1994), CERN 94-03, pp. 411–415.
- [6] J. Bosser *et al.*, *Part. Accel.* **63** (1999) 171.
- [7] K. Schindl, Ion injector issues, Proc. Twelfth Chamonix Workshop on LHC Performance, Chamonix, France, 2004, Ed. J. Poole (CERN, Geneva 2003), p. 64.
- [8] M. Benedikt *et al.* (Eds), LHC design report, CERN-2004-003-V-3 (2004), pp. 263–356.
- [9] C. Carli *et al.*, LEIR: towards the nominal lead ion beam, Proc. Fourth Asian Particle Accelerator Conf., Indore, India, 2007 (JACoW, Geneva, 2007), TUPMA085.
- [10] M. Chanel, LEAR performance, CERN-PS-99-040-DI (1999).
- [11] D. Möhl, LEAR, history and early achievements, CERN-PS-99-034-DI (1999).
- [12] C. Carli *et al.*, LEIR commissioning, Proc. Tenth European Particle Accelerator Conf., Edinburgh, Scotland, 2006, Eds. C. Biscari, H. Owen, C. Petit-Jean-Genaz, and J. Poole (JACoW, Geneva, 2006), p. 1876.
- [13] C. Carli *et al.*, LEIR Lattice, Proc. Tenth European Particle Accelerator Conf., Edinburgh, Scotland, 2006, Eds. C. Biscari, H. Owen, C. Petit-Jean-Genaz and J. Poole (JACoW, Geneva, 2006), p. 261.
- [14] G. Tranquille, Electron cooling experiments at LEIR, Proc. Eleventh European Particle Accelerator Conf., Genoa, Italy, 2008, Eds. C. Biscari and C. Petit-Jean-Genaz (JACoW, Geneva, 2008), THPP057.
- [15] G. Tranquille *et al.*, Cooled beam diagnostics on LEIR, Proc. Eleventh European Particle Accelerator Conf., Genoa, Italy, 2008, Eds. C. Biscari and C. Petit-Jean-Genaz (JACoW, Geneva, 2008), TUPC102.

- [16] C. Bal *et al.*, LEIR beam instrumentation, Proc. Seventh European Workshop on Beam Diagnostics and Instrumentation for Particle Accelerators, Lyon, France, 2005 (JACoW, Geneva, 2005), p. 57.
- [17] G. Baur *et al.*, Phys. Lett. **B368** (1996) 251.
- [18] S. van der Meer, Stochastic Extraction, a Low Ripple Version of Resonant Extraction, CERN-PS-AA-78-6 (1978).
- [19] R. Capii, W. Hardt and C. Steinbach, Ultra slow extraction with good duty factor, Proc. Eleventh Int. Conf. on High-Energy Accelerators, Geneva, Switzerland, 1980, Ed. W.S. Newman (Birkhäuser, Basel, 1980), p. 335.
- [20] A. Wolf *et al.*, Nucl. Instrum. Methods Phys. Res. **A441** (2000) 183.
- [21] H. Danared *et al.*, Phys. Rev. Lett. **86** (2001) 5027.
- [22] N. Madsen, Vacuum Changes during Accumulation of Pb⁵⁴⁺ in LEIR, PS/DI Note 99-21 (1999).
- [23] E. Mahner *et al.*, Molecular Desorption of Stainless Steel Vacuum Chambers Irradiated with 4.2 MeV/u Lead Ions, CERN-LHC-Project-Report-624 2003 [*Phys. Rev. ST Accel. Beams* **6** (2003) 013201].
- [24] C. Carli, S. Maury and D. Möhl, Combined longitudinal and transverse multiturn injection in a heavy ion accumulator, Proc. Seventeenth Particle Accelerator Conf., Vancouver, Canada, 1997, Eds. M. Comyn, M.K. Craddock, M. Reiser and J. Thomson (IEEE, Piscataway, NJ, 1998), p. 976.
- [25] G. Tranquille *et al.*, Commissioning of the LEIR electron cooler with Pb⁵⁴⁺ ions, Proc. Twentieth Russian Conf. on Charged Particle Accelerators, Novosibirsk, Russia, 2006 (JACoW, Geneva, 2006), WEBO01.
- [26] J. Pasternak *et al.*, A collimation scheme for ions changing charge state in the LEIR ring, Proc. Twenty First Particle Accelerator Conf., Knoxville, Tennessee, 2006, Eds. M. Arena, J. Chrin, M. Comyn, C. Eyberger, C. Horak, L. Liljeby, M. Marx, H. Owen, J. Patton and C. Petit-Jean-Genaz (JACoW, Geneva, 2006), p. 3816.
- [27] B. Franzke, Review of heavy ion storage rings, Proc. Third European Particle Accelerator Conf., Berlin, Germany, 1992, Eds. H. Henke, H. Homeyer, and C. Petit-Jean-Genaz (Ed. Frontières, Gif-sur-Yvette, 1992), p. 367.

The LEP Pre-Injector (LPI)

1 Introduction

The studies for a very Large Electron–Positron collider (LEP) started in 1975 at CERN. Very soon attention was given also to its injector and the focus was on a new purpose-built 15 GeV to 22 GeV synchrotron fed by a small accumulation ring preceded by a tandem of linear accelerators (linacs). A collaboration with the Laboratoire d’Accélérateur Linéaire (LAL) in Orsay, France was formed for the design of this pre-injector in order to draw from the experience of LAL with e^+e^- accelerators. LAL contributed with preliminary conceptual designs for the linacs and the accumulation ring.

In 1980 the use of the Super Proton Synchrotron (SPS) and Proton Synchrotron (PS) as lepton injectors was proposed providing a substantial saving compared with a new synchrotron. As the pre-injector was now linked to the PS it was most logical that the PS Division became responsible for this set of new accelerators with LAL as a partner. The collaboration with LAL was formalized in 1982 with an agreement concentrating the expertise from LAL on the design, construction and running-in for the linacs, the PS Division took full responsibility for the accumulation ring and the beam transfer to the PS as well as for the required modifications in the PS ring.

The front-end of the high-current linac (gun, prebuncher and S-band buncher) was the first element ordered and was installed in 1981 at LAL in order to study the output beam quality in detail. In 1986, both S-band linacs operated at design energy and the accumulation ring was installed allowing it to be tested with electrons. In 1987, the pre-injector was fully operational and ran for 2200 h providing the PS with both types of particles for acceleration to 3.5 GeV.

2 Baseline design

The LEP Pre-Injector (LPI) consisted of the LEP Injector Linacs (LIL) and the Electron-Positron Accumulation ring (EPA) [1]. The intense 200 MeV e^- beam (2.5 A peak) of the first linac (LIL-V) in the tandem produced the e^+ beam in a converter target upstream of the 600 MeV low-intensity linac (LIL-W). The electrons for the e^- filling of LEP were produced by a low-intensity gun located near the converter.

The high-current front-end of LIL-V consisted of a 90 keV e^- gun, a prebuncher cavity and a SW tri-periodic buncher with 33 MeV non-load energy gain. It was followed by four S-band accelerating sections driven by one 35 MW klystron which was equipped with a RF pulse compression system, called the LIL Power Saver (LIPS), based on the SLAC Energy Doubler (SLED) scheme. The non-load energy of LIL-V was 225 MeV.

The 6 m long section between the two linacs housed a spectrometer line for the high-current beam, the conversion target, the low-current e^- gun and its associated 4 MeV buncher.

LIL-W consisted of 12 S-Band accelerating sections where the first two and the last two accelerating sections were driven by one klystron. Two klystrons with LIPS provided the power to the two middle groups of four sections. Each klystron provided a maximum power of 35 MW in 4.5 μ s at 2998 MHz ($\lambda = 10$ cm).

The accelerating sections of both linacs were identical consisting of 4.5 m long disc-loaded waveguides operating in travelling-wave mode with a $2\pi/3$ phase advance and containing 135 cells. In order to reduce the number of different cell types required compared with a constant gradient structure, the section consisted of 9 constant-impedance landings with 11 identical cells per landing, except the input and output landings which had 13 cells. Four transition cells between the landings reduced the reflections of the electromagnetic wave. The average gradient was 12 MV/m. With LIPS compressing the 4.5 μ s long RF pulse to the filling time 1.2 μ s of the section, the energy gain per section could be increased by a factor of 1.6.

Quadrupoles provided beam focusing in the linacs. The positron converter was followed by a short pulsed solenoid and two solenoids on the first accelerating sections of LIL-W. Figure 1 gives a view of the LIL-V and LIL-W.

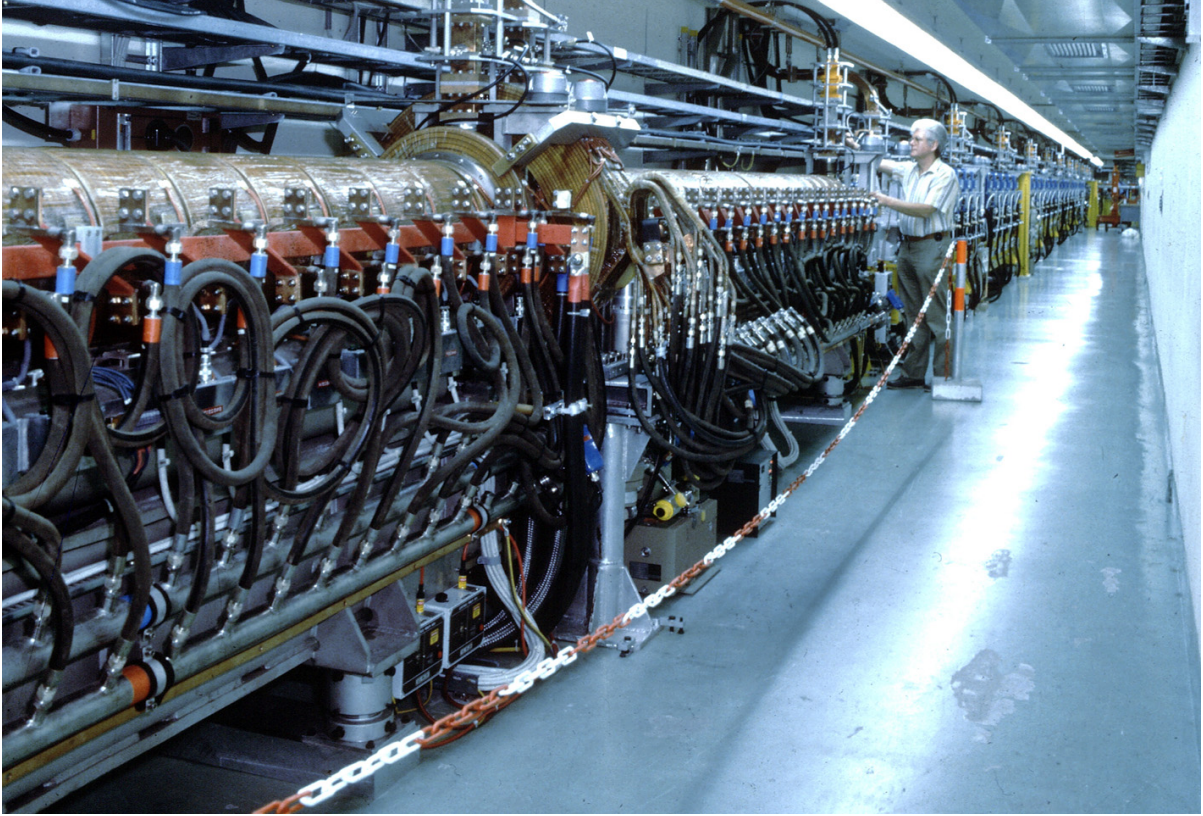


Fig. 1: Looking downstream from the second accelerating section of LIL-W towards LIL-V. The two accelerating structures of LIL-W are not visible as embedded in solenoids. The man is standing near the converter target between LIL-V and LIL-W.

The circumference of EPA was grossly determined by the requirement that its kicker magnets should independently handle each of the eight bunches circulating in EPA. The circumference of EPA (125.7 m) was exactly one fifth of the PS to allow for beam transfer within one PS turn.

The eight combined-function bending magnets per arc provided horizontal damping ($J_x = 2$) to enhance injection efficiency. In turn, the damping of energy oscillation ($J_e = 1$) was reduced resulting in a larger energy spread, welcome for bunch stability. The bending magnets were relatively short in order to enhance radiation damping resulting in a fairly high magnetic field (1.4 T). The gradient in the magnets was -1 T/m. The quadrupoles producing the required focusing in the straight sections and additional focusing in the arcs had been taken from the Intersecting Storage Rings (ISR) which was closed at the end of 1983. Figure 2 shows part of an arc of EPA and a straight section in the background.

A single capacitive loaded RF cavity of the quarter-wave-length type driven by one tetrode provided 50 kV. It operated at 19.1 MHz corresponding to harmonic number eight. Thus, eight buckets were available to build up the eight bunches. The cavity had a passive damping system for higher-order modes. The conventional vacuum system maintained a vacuum of around $1 \mu\text{Pa}$. This was determined more by the desire to avoid ion trapping than dictated by the required lifetime of the beam, being only about 10 s in the ring.



Fig. 2: Arc and straight section of the EPA. Red: bending magnets; blue: quadrupoles; yellow: sextupoles. The white vertical and horizontal tubes above the arc guided the light to the synchrotron radiation monitor.

The vacuum system had also to cope with the degassing by the synchrotron radiation which had only a critical energy of 0.33 keV and, therefore, was completely absorbed by the stainless steel vacuum chamber.

A suitable location near the PS was found for LPI after the neutrino tunnel, which contained the beam lines for Gargamelle, and its associated power supply building had been demolished. However, use was made of the three existing buildings which were before the g-2 experimental hall, the Gargamelle cooling room and the East Hall power supply building. The two linacs together had a total length of about 100 m and their position was radial to the PS with LIL-W extending under the racetrack-shaped EPA ring to achieve a compact layout. The klystron gallery was superimposed on the LIL tunnel. The EPA building had the weird racetrack shape of EPA which will severely limit its future use for other purposes, diverging from the good tradition at CERN. Only the roof shielding had to be incorporated into the building structure, all lateral shielding was provided by shielding blocks becoming available from the CERN West Experimental Area, which resulted in significant savings.

3 Operation

The electrons and the positrons had to be accelerated in the SPS in its dead-time during its fixed-target proton operation. Four e-acceleration cycles of the synchrotrons were fitted in this dead-time: the first two for e^+ acceleration, the latter for e^- acceleration. Hence, both beams in LEP were built up nearly simultaneously to keep the RF beam loading and the space charge detuning about equal for both beams. The dead-time was imposed by the limit on the average power consumption of the SPS accelerating protons to 450 GeV. The four e-cycles to 20 GeV were admissible as they had a negligible impact on this power consumption.

EPA worked as a buffer between the slow-cycling synchrotrons (1.26 s repetition time of the PS, 15.2 s for the SPS) and the linacs operating at 100 Hz. Since the e^+ peak current (8 mA) from the LIL-W was much lower than the e^+ peak current (40 mA), the e^+ were collected in EPA for 11 s during the long SPS proton cycle. Here peak current stands for average current during a linac pulse. The linac pulses were put into eight equally spaced EPA buckets by stacking in betatron phase space. The time elapsing between two injections into the same bucket was 80 ms, sufficiently long compared with the EPA damping time ($\tau_x = 30$ ms).

At the end of the accumulation each of the eight e^+ bunches was moved onto a thin electrostatic septum cutting the bunch into two halves and deflecting one half into the transfer channel to the PS. The other eight halves remained in EPA and were saved for the next e^+ cycle. They were ejected 1.26 s later. Then the e^- were accumulated in eight buckets for 1.14 s for the first e^- batch followed by the accumulation of the second e^- batch before e^+ injection was resumed.

4 Evolution

All numerical values given in the preceding paragraph are the design values. Many parameters were later modified and adapted in light of the experience and hardware constraints in order to optimize operation.

In 1987, the first year of routine operation, the LPI performance [2] exceeded the design specifications [1] except for positron production where design figures were reached in the following year and EPA which had to operate at 500 MeV. A number of voltage-related weak points in the modulator/klystron assemblies was not solved and it was preferred to operate LIL-W and EPA below the design energy of 600 MeV resulting in a longer but acceptable damping time ($\tau_x = 58$ ms).

The 600 MeV level was reached in 1988 but the energy was decreased later again to 500 MeV in routine operation to gain in reliability. In the same year the operation had been simplified. Both types of beams were now produced with the gun of LIL-W properly modulated and by using a converter target with a 5 mm diameter hole moved onto the beam axis during the e^- cycle. Some mismatch of the e^- beam to LIL-W had to be accepted as the LIL-V focusing could not be changed from cycle to cycle. The energy of e^- beam was controlled by adjusting the phases and timings of LIPS which could be modulated with the required speed. The e^- gun of LIL-W and the buncher were removed.

In 1990, the LIL-V front-end was improved with a new gun pulser (maximum 100 kV, routine 80 kV) and a shorter 4 MeV buncher replacing the original which freed space for a better matching system to the upstream linac section. The positron conversion system was further simplified. The electron beam was deflected through a 2.5 mm diameter hole beside the 5 mm diameter W-target by means of three deflecting magnets. Hence, the converter could stay in a fixed position. The overall performance of LPI exceeded the design performance by a factor of three for e^+ and a factor of five for e^- (see Refs. [3, 4]).

Since it turned out that the downstream synchrotrons could accelerate the nominal bunch intensity twice easily, the supercycle of the LEP injection chain lasting 14.4 s was simplified from

1994 onwards. Only one e^+ cycle and one e^- cycle were used to fill LEP with the advantage that 2.4 s became available for cycles serving other users either of PS or SPS and slicing of the e^+ bunches in EPA could be eliminated. The PS cycle had been shortened from 1.26 s to 1.20 s.

The availability of LPI reached a first peak with more than 95% from 1989 until 1991 but degraded afterwards a little due to the aging of the klystrons but never fell below 93%. A sustained consolidation programme resulted in 98% in the last runs from 1997 to 2000.

LPI not only served as a reliable pre-injector for LEP but its beams were used in the time between the LEP fills for a number of experiments. The most spectacular was the production of single electrons between 180 MeV and 500 MeV for calibration of the BGO crystals for the LEP L3 experiment. The beam intensity was reduced by slits in the LIL-EPA transfer line and EPA was used as a spectrometer. The electrons were ejected after 1(1/4) turn into a new short transfer line to the test area in a small extension of the EPA hall [5]. Since the synchrotron radiation spectrum at 345 MeV was very close to that expected for protons at 8 TeV in the LHC, two photon beam lines branching off from EPA had been set up for the irradiation of the LHC sample vacuum and cryogenic equipment [6]. This activity continued in 2001 after the closure of LEP when in addition the production of neutron-rich radioactive nuclei through photoemission was studied. The photons were produced by bremsstrahlung in a W-target hit by 50 MeV electrons from LIL [7].

5 Conclusion

Although CERN had no experience with electron linacs or electron rings, it managed with the help of LAL/Orsay to design and construct LPI within about 5 years. Thanks to prudently chosen parameters and careful commissioning, the required performance could be reached rather quickly, so that the synchrotrons downstream in the injector chain, conceived as proton accelerators, could be commissioned with e^+ and e^- in time for the LEP arc test in 1988 which preceded the start of LEP operation in 1989.

LPI remained a reliable pre-injector for LEP thanks to a practically continuous consolidation of equipment until the closure of LEP in 2000. In addition, it served a number of experiments before LPI was transformed to become the CLIC Test Facility (CTF). This development for CTF started in 1999 when the EPA lattice was temporarily modified to test isochronous operation in view of the future use of EPA as a combiner ring. This conversion of LPI is another example of traditional husbandry of CERN making use of resources from a former project for research and development possibly leading to a next stage.

References

- [1] The LEP Injector Study Group, The LEP Injector Chain, LEP Design Report Vol. I, CERN/PS/DL/83-31 and LAL/RT/83-09 (1983).
- [2] J. H. B. Madsen *et al.*, First experience with the LEP Pre-Injector (LPI) by the LPI beam commissioning team, Proc. Twelfth IEEE Particle Accelerator Conf., Washington, DC, 1987 (IEEE, New York, 1987), p. 298.
- [3] S. Battisti *et al.*, Progress report on the LEP Pre-injector, in Proceedings of the Thirteenth IEEE Particle Accelerator Conference, Chicago, USA, 1989, edited by F. Bennett and J. Kopta (IEEE, New York, 1989), p. 1815.
- [4] R. Bossart *et al.*, The LEP Injector Linac, CERN/PS 90-56 (LP) (1990).
- [5] B. Frammery *et al.*, Single electron beams from the LEP Pre-Injector, Proc. Thirteenth IEEE Particle Accelerator Conf., Chicago, IL, 1989, Eds. F. Bennet and J. Kopta (IEEE, New York, 1989), p. 289.
- [6] V.V. Anashin *et al.*, *Vacuum* **60** (2001) 15.
- [7] S. Essabaa *et al.*, *Nucl. Instrum. Methods Phys. Res.* **B204** (2003) 780.

Linac 3

1 Introduction

After the successful experiments with light ions delivered from Linac 1, and due to the impossibility of an upgrade towards heavier ions, a study was launched to analyse the options for a new linear accelerator (linac) that could deliver heavy ions [1]. Taking into account the state of the art for source technology of the time, restrictions from the other machines and the interest from the high-energy physics community, a linac accelerating lead ions (Pb^{25+}) up to an energy of 4.2 MeV/u and followed by a stripping stage delivering Pb^{53+} was feasible in the hall where Linac 1 was installed, for injection into the Proton Synchrotron Booster (PSB).

The project was realized within an international collaboration [2]. CERN delivered the infrastructure and the 200 MHz RF system, GANIL, Caen delivered the source, INFN Legnaro produced the Low Energy Beam Transport (LEBT), the Radiofrequency Quadrupole (RFQ) and the Medium Energy Beam Transport (MEBT), GSI Darmstadt made the 100 MHz RF system and the Interdigital H (IH) linac, INFN Torino delivered the High Energy Beam Transport (HEBT) including the ion filter line, and IAP Frankfurt delivered the debuncher. Additional assistance was given by the Czech Republic, India, Sweden and Switzerland.

2 Machine layout

The ion beam was produced by an Electron Cyclotron Resonance Ion Source (ECRIS), version ECR4 [3] (Fig. 1). The ions are created in a microwave-heated plasma, with the source running in a so-called “afterglow” mode [4]. The microwave power to the source (14.5 GHz) is pulsed with a 10 Hz repetition rate and 50 ms pulse length. The peculiarity of the afterglow mode is that after the microwave pulse is switched off, a short intense pulse of medium and highly charged ions can be extracted from the source. The isotopically pure lead ^{208}Pb is evaporated in a micro-oven inside the source and ionized in an oxygen-supported plasma.

The ions are extracted from the source with an energy of 2.5 keV/u and in the LEBT the mixture of lead charge states (as well as the oxygen beam) is separated in a 135° spectrometer, after which the beam is adapted for the injection into the RFQ with a pair of solenoids and a quadrupole triplet. In the design a lead charge state of Pb^{25+} was foreseen, but after some operational experience Pb^{27+} was chosen as a slightly higher intensity was available, but more importantly it allowed the following RF structures to run with a lower RF field level, lowering the amount of X-rays generated.

The RFQ accelerates the ions from 2.5 keV/u to 250 keV/u. It is 2.66 m long and operates at a frequency of 101.28 MHz. In the following MEBT, four magnetic quadrupoles match the beam to the accelerating tanks and a four-gap RF cavity matches the longitudinal bunch parameters.

For the rest of the acceleration up to 4.2 MeV/u (requiring about 30 MV of accelerating voltage) a three-cavity IH structure was chosen [5]. The first cavity operates at the same frequency as the RFQ (101.28 MHz), but the second and third cavities operate at a frequency of 202.56 MHz, with the total length of this accelerating region being 8.13 m. Four quadrupole triplets are installed for the beam focussing, two in cavity 1 and one between each cavity.

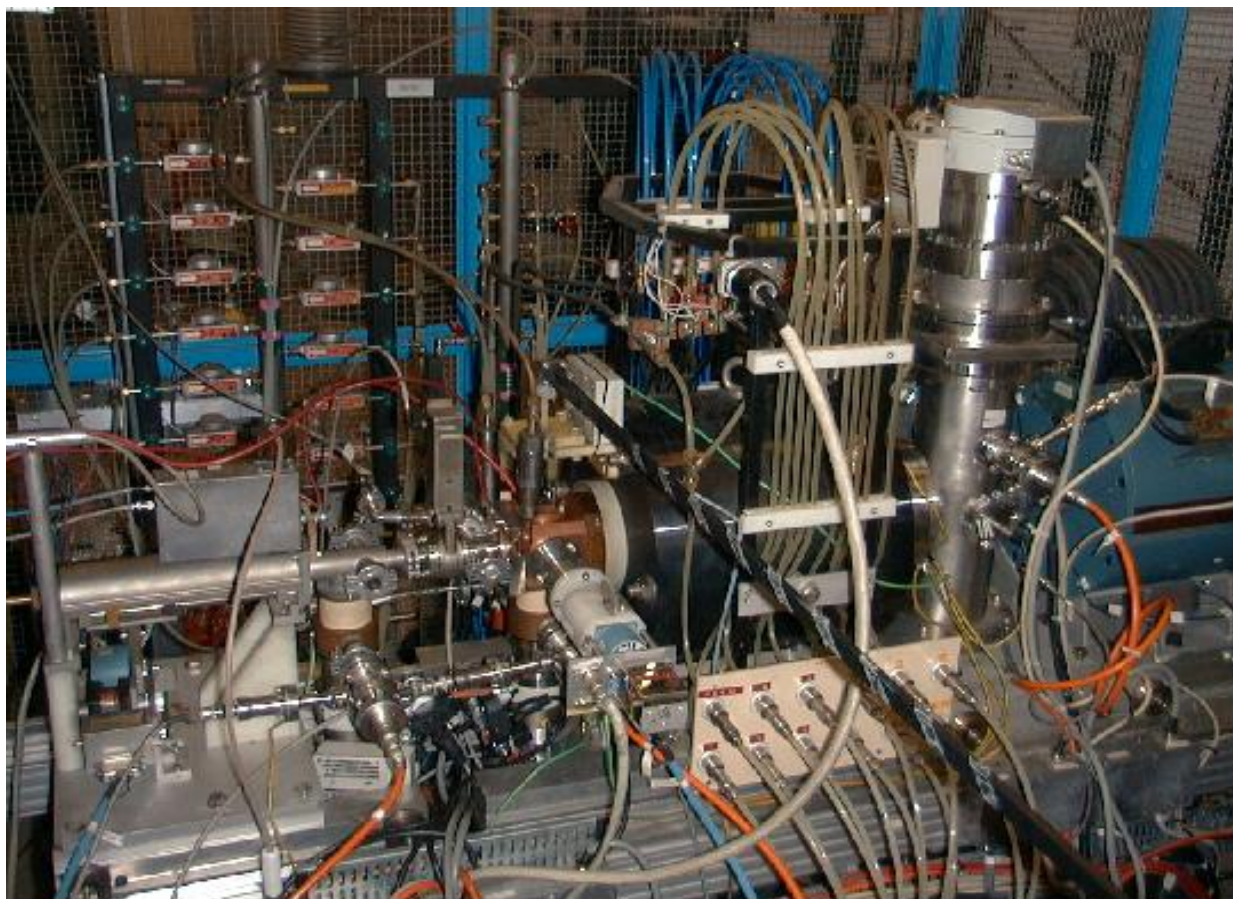


Fig. 1: ECR4 ion source

After the linac follows the Linac-to-Filter (ITF) line for measurements, stripping and filtering. The stripper comprises an annealed carbon foil of $100 \mu\text{g}/\text{cm}^2$ is used, from which roughly 18% of the beam emerges with the design charge state of Pb^{53+} . The other charge states are filtered out in the filter line.

The ITF line joins the transfer line of Linac 2 inside the Proton Synchrotron (PS) tunnel for the injection into the PSB.

The construction of Linac 3 began in October 1992, after removing Linac 1 from the accelerator hall. After only 20 months in May/June 1994 the beam was commissioned in the linac and then sent to the PSB on 15 June 1994, with the nominal beam intensity at the PSB injection point being available just a few days later.

The only component that was not available for this start-up was the 101 MHz RF system, for which GSI provided a temporary solution by modifying two 108 MHz amplifier systems and installing them at CERN. These were replaced the following year with a new commercially built system.

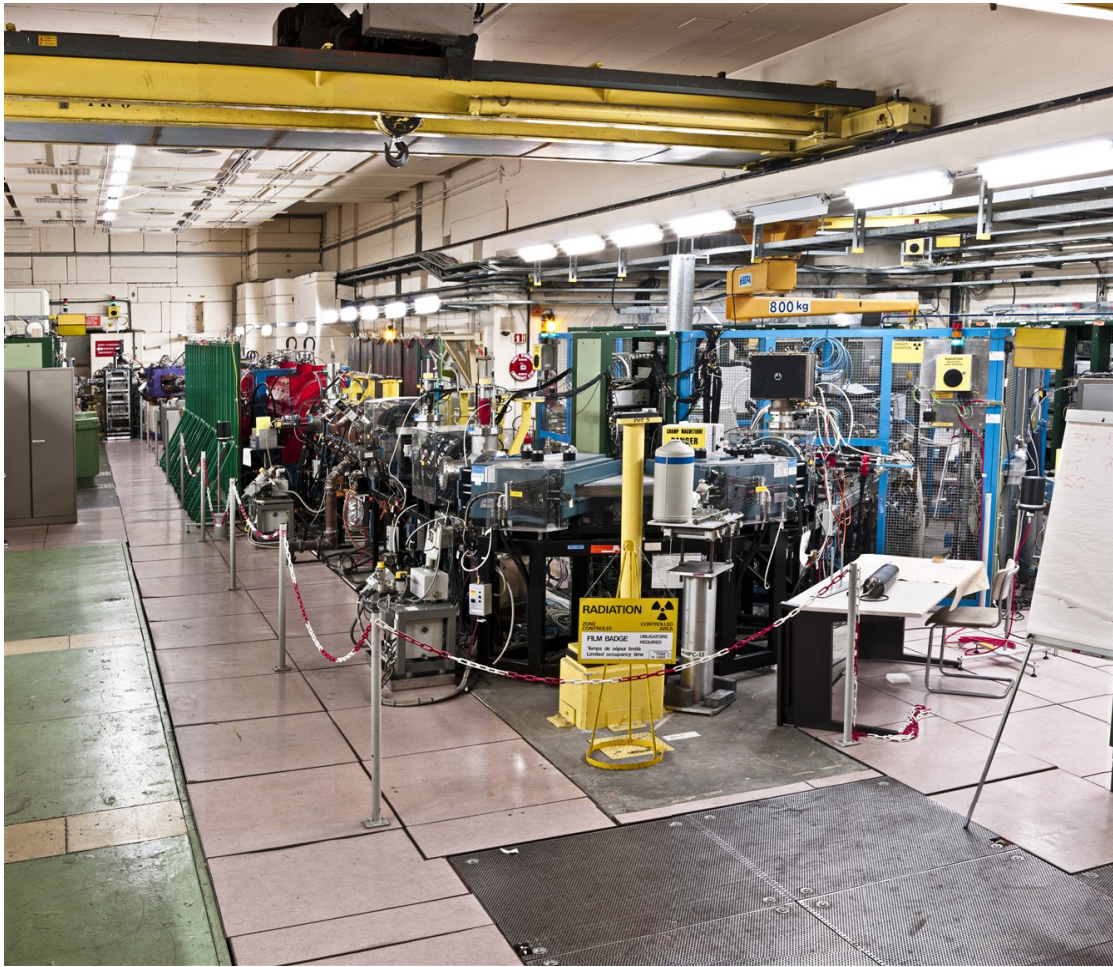


Fig. 2: Linac 3: right-hand side, in the cage, the source; in front, the spectrometer; and left-hand side, the RFQ and the accelerating tanks.

3 Operation for the Super Proton Synchrotron fixed target programme

The linac was delivering beam for the Super Proton Synchrotron (SPS) fixed target physics programme from 1994 until 2003, except 1997 and 2001. In the years between 1994 and 2002 a lead beam was provided. In 2003 an indium beam was delivered for SPS fixed target experiments. At the source this could be produced from metallic indium evaporated from the filament heated oven.

Compared with the proton operation which is running nearly the whole year, the heavy ions were requested only during a period of 6–8 weeks in the Autumn of each year.

The source delivered typically (70–80) μA of Pb^{27+} in a 650 μs long pulse (measured after the RFQ), which resulted in (20–24) μA of Pb^{53+} at the end of the linac. The repetition rate of the linac was 0.8 Hz. The linac already produced the nominal intensity for the first fixed target ion run in 1994, and after this there were only small incremental increases in the performance. Development work concentrated on improving the reliability of the accelerator and the stability of the beam.

Since 2000 a vacuum desorption experiment [6] was installed at the end of the linac. The aim was the measurement of gas desorption rates from different vacuum chamber surfaces. The results of these experiments were used for the design of the vacuum system of the Low Energy Ion Ring (LEIR).

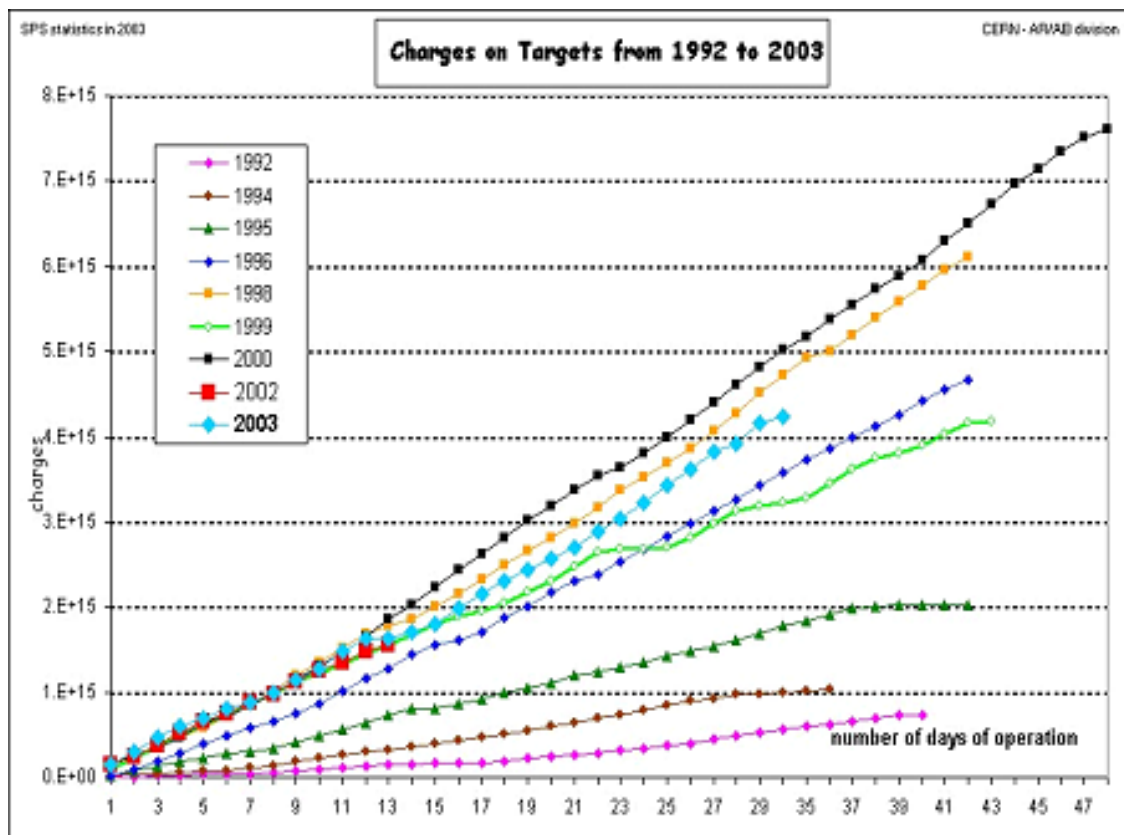


Fig. 3: Operational statistics for the years 1992–2003. The number of charges on the SPS target are shown.

4 Modifications and operation for the Large Hadron Collider heavy-ion physics programme

Linac 3 and the PSB could only deliver a beam with 1/30 of the brightness required for collisions in the Large Hadron Collider (LHC) and, even at its design, components were specified for eventual operation at 10 Hz to allow the operation of accumulation and cooling in a dedicated ring. In the early 2000s the situation was reviewed and several options to overcome this problem were discussed, for example upgrading the present source to a higher microwave frequency, replacing the source with another source type (electron beam ion source or laser ion source) as well as the conversion of the Low Energy Antiproton Ring (LEAR) into an ion accumulator. Finally it was decided to renovate LEAR (at the same time changing its name to LEIR) as well as to copy an existing electron cyclotron resonance (ECR) source, the Grenoble Test Source (GTS), developed and built by CEA, Grenoble, which proved to be able to deliver the requested beam parameters [7].

With the new source, called GTL-LHC [8, 9], the current out of the RFQ could be increased to (100–120) μA of Pb^{29+} , which results in around 25 μA of Pb^{54+} at the end of the linac. The pulse length was shortened for the injection into LEIR to 200 μs , whereas the repetition rate of the linac is now between 0.8 Hz and 5 Hz, depending on the injection scheme. As higher repetition rates were foreseen for Linac 3 already at its design stage, only some pulsed quadrupole magnets required new power converters, as well as some necessary small cooling modifications along the linac.

The charge state from the source was further increased to Pb^{29+} to be able to reduce the fields in the RF tanks and to lower in this way the radiation in the hall and so allowing the higher repetition rate of the linac. Pb^{54+} out of the linac is now used due to the higher lifetime of this charge state in LEIR compared with Pb^{53+} .

Another necessary modification of the linac was the installation of a ramping cavity after the stripper. For the injection into LEIR a 3D phase space painting is used. The ramping cavity is used to provide the energy variation during the pulse for the longitudinal painting.

The new source was ordered in 2004 and installed and commissioned in the beginning of 2005. For the first commissioning of LEIR, a oxygen beam was used to allow initial commissioning without the expected strong ion desorption effect in LEIR and as the newly commissioned source was more stable in this mode.

Since then until 2009 the new source and the modified linac with the new operational settings were used for the commissioning of the accelerator chain for the LHC heavy-ion programme. In 2010 the first heavy-ion collisions took place in the LHC.

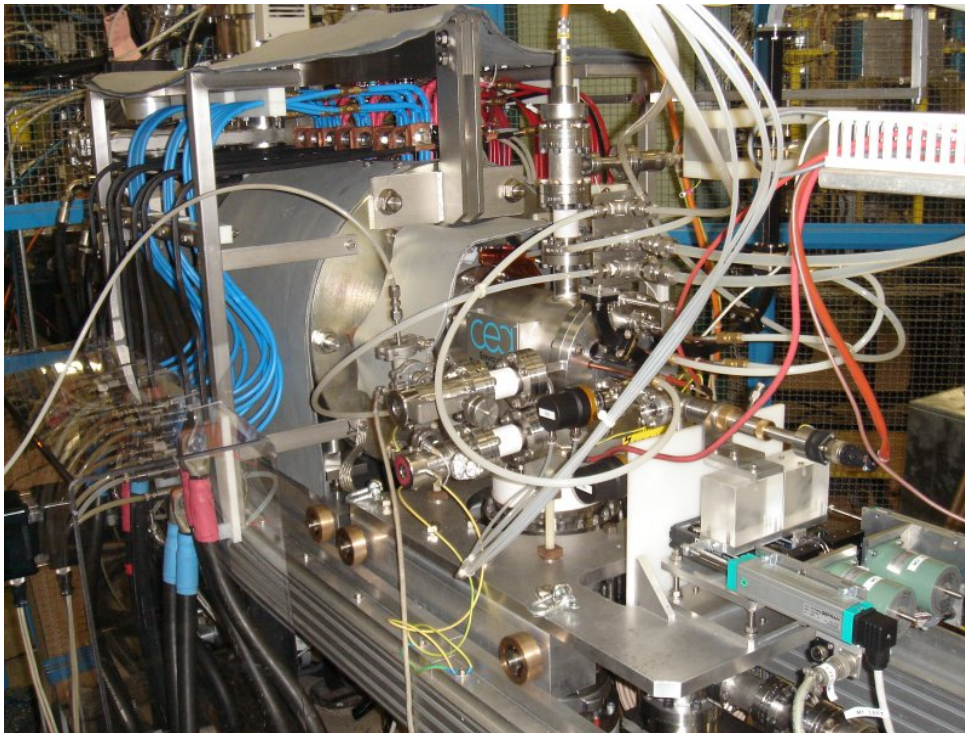


Fig. 4: GTS-LHC ion source

5 Conclusions

Linac 3 fulfilled the expectations of an injector for a heavy-ion facility. It was running successfully for the period of SPS heavy-ion fixed target physics and with some modifications it has now started to serve the LHC heavy-ion programme.

In combination with the LEIR ring Linac 3 is not only restricted to heavy ions such as lead. SPS fixed target experiments such as NA61 request now also lighter ions such as argon and xenon. In addition to all of this completely new clients have reported their interest in the use of light-ion beams

in the CERN injector complex. In the future radiobiological and space science experiments may also be served from Linac 3.

References

- [1] H. Haseroth (ed.), Concept for a Lead-Ion Accelerating Facility at CERN, CERN 90-01 (1990).
- [2] D. Warner (ed.), CERN Heavy-Ion Facility Design Report, CERN 93-01 (1993).
- [3] C.E. Hill and K. Langbein, *Rev. Sci. Instrum.* **69** (1998) 643.
- [4] C.E. Hill and K. Langbein, *Rev. Sci. Instrum.* **67** (1996) 1328.
- [5] N. Angert et al., The IH Linac of the CERN Lead Injector, Proc. Linac94, Tsukuba, Japan, p. 753.
- [6] E. Mahner, *Phys. Rev. ST Accel. Beams* **11** (2008) 104801.
- [7] D. Hitz *et al.*, Grenoble Test Source (GTS): a multipurpose room temperature ECRIS, Proc. 15th Int. Workshop on ECR Sources, Jyväskylä, 2002, JYFL Research Report 4/2002, 2002.
- [8] C.E. Hill, D. Kuchler, C. Mastrostefano, M. O'Neil, R. Scrivens, D. Hitz, L. Guillemet, J. Chartier, J.-M. Mathonnet and G. Rey-Giraud., Experience with the GTS-LHC Ion Source, LHC Project Workshop - Chamonix XV, January 2006.
- [9] L. Dumas, C. Hill, D. Hitz, D. Kuchler, C. Mastrostefano, M. O'Neil and R. Scrivens, Operation of the GTS-LHC Source for the Hadron Injector at CERN, Proc. 17th Int. Workshop on ECR Ion Sources and Their Applications, Lanzhou, China, 17–21 September 2006, pp. 51–54.

